THE JOURNAL OF IMMUNOLOGY

Suppressor of Cytokine Signaling 1 DNA Administration Inhibits Inflammatory and Pathogenic Responses in Autoimmune Myocarditis

Kazuko Tajiri, Kyoko Imanaka-Yoshida, Akihiro Matsubara, Yusuke Tsujimura, Michiaki Hiroe, Tetsuji Naka, Nobutake Shimojo, Satoshi Sakai, Kazutaka Aonuma and Yasuhiro Yasutomi

J Immunol 2012; 189:2043-2053; Prepublished online 13 July 2012;
doi: 10.4049/jimmunol.1103610
http://www.jimmunol.org/content/189/4/2043

The Journal of Immunology is published twice each month by
The American Association of Immunologists, Inc.,
9650 Rockville Pike, Bethesda, MD 20814-3994.

Print ISSN: 0022-1767 Online ISSN: 1550-6606.

Suppressor of Cytokine Signaling 1 DNA Administration Inhibits Inflammatory and Pathogenic Responses in Autoimmune Myocarditis

Kazuko Tajiri,*,† Kyoko Imanaka-Yoshida,‡,§ Akihiro Matsubara,*,¶ Yusuke Tsujimura,* Michiaki Hiroe,‖ Tetsuji Naka,# Nobutake Shimojo,† Satoshi Sakai,† Kazutaka Aonuma,† and Yasuhiro Yasutomi*,¶

Myocarditis and subsequent dilated cardiomyopathy are major causes of heart failure in young adults. Myocarditis in humans is highly heterogeneous in etiology. Recent studies have indicated that a subgroup of myocarditis patients may benefit from immune-targeted therapies, because autoimmunity plays an important role in myocarditis as well as contributing to the progression to cardiomyopathy and heart failure. Suppressor of cytokine signaling (SOCS) 1 plays a key role in the negative regulation of both TLR- and cytokine receptor-mediated signaling, which is involved in innate immunity and subsequent adaptive immunity. In this study, we investigated the therapeutic effect of SOCS1 DNA administration on experimental autoimmune myocarditis (EAM) in mice. EAM was induced by s.c. immunization with cardiac-specific peptides derived from α myosin H chain in BALB/c mice. In contrast to control myocarditis mice, SOCS1 DNA-injected mice were protected from development of EAM and heart failure. SOCS1 DNA administration was effective for reducing the activation of autoreactive CD4$^+$ T cells by inhibition of the function of Ag-presenting dendritic cells. Our findings suggest that SOCS1 DNA administration has considerable therapeutic potential in individuals with autoimmune myocarditis and dilated cardiomyopathy. ***The Journal of Immunology*****, 2012, 189: 2043–2053.**

Dilated cardiomyopathy (DCM) is a potentially lethal disorder of various etiologies for which no treatment is currently satisfactory (1); it often results from enteroviral myocarditis (2, 3). Many patients show heart-specific autoantibodies (3, 4), and immunosuppressive therapy can improve cardiac function in DCM patients who show no evidence of viral or bacterial genomes in heart biopsy samples (5). These observations suggest that autoimmunity plays an important role in myocarditis as well as contributing to the progression to cardiomyopathy and heart failure (6).

Experimental autoimmune myocarditis (EAM) is a model of postinfectious myocarditis and cardiomyopathy (7). A number of proinflammatory cytokines, including IL-1β, IL-6, IL-12, TNF-α, and GM-CSF, have been shown to contribute to the development of autoimmune myocarditis in animal models and human cases (8–13). EAM is a CD4$^+$ T cell-mediated disease (7, 14), and activation of self-Ag–loaded dendritic cells (DCs) is critical for expansion of autoreactive CD4$^+$ T cells. Activation of TLRs and IL-1 type 1 receptor and their common downstream signaling adaptor molecule, MyD88, in self-Ag–presenting DCs is also critical for the development of EAM (11, 15, 16). Compared with inhibition of a single cytokine, a more effective treatment might be inhibition of various signaling pathways to induce production of cytokines through both innate and adaptive immunity. One strategy that could accomplish this would be to target shared cytokine and TLR signal transduction pathways using suppressor of cytokine signaling (SOCS) molecules.

Recent lines of evidence indicate that SOCS proteins, originally identified as negative-feedback regulators in cytokine signaling, are involved in the regulation of TLR-mediated immune responses (17, 18). The SOCS family is composed of eight members: cytokine-inducible Src homology 2 domain-containing protein and SOCS1 to SOCS7 (19, 20). SOCS1 plays a key role in the negative regulation of both TLR-mediated signaling and cytokine receptor-mediated signaling, which are involved in innate immunity and subsequent adaptive immunity (21). The expression of SOCS1 is induced by various cytokines, including IFN-γ, IL-4, and IL-6, and also by TLR ligands, such as LPS and CpG-DNA (22). Several studies have demonstrated that SOCS1 is a negative regulator of LPS-induced macrophage activation and plays an essential role in suppression of systemic autoimmunity mediated by DCs (23–25). Thus, SOCS1 regulates not only adaptive immunity

*Laboratory of Immunoregulation and Vaccine Research, Tsukuba Primate Research Center, National Institute of Biomedical Innovation, Tsukuba, Ibaraki 305-0843, Japan; †Department of Cardiovascular Medicine, Majors of Medical Sciences, Graduate School of Comprehensive Human Sciences, University of Tsukuba, Tsukuba, Ibaraki 305-8575, Japan; ‡Department of Pathology and Matrix Biology, Mie University Graduate School of Medicine, Tsu, Mie 514-8507, Japan; §Mie University Matrix Biology Research Center, Mie University Graduate School of Medicine, Tsu, Mie 514-8507, Japan; ¶Division of Immunoregulation, Department of Molecular and Experimental Medicine, Mie University Graduate School of Medicine, Tsu, Mie 514-8507, Japan; ‖Department of Cardiology, National Center for Global Health and Medicine, Shinjuku, Tokyo 162-8655, Japan; and #Laboratory of Immune Signal, National Institute of Biomedical Innovation, Ibaragi, Osaka 565-0871, Japan

Received for publication December 13, 2011. Accepted for publication June 5, 2012.

This work was supported by Health Science Research grants from the Ministry of Health, Labor and Welfare of Japan and the Ministry of Education, Culture, Sports, Science and Technology of Japan.

Address correspondence and reprint requests to Dr. Yasuhiro Yasutomi, Laboratory of Immunoregulation and Vaccine Research, Tsukuba Primate Research Center, National Institute of Biomedical Innovation, 1-1 Hachimandai, Tsukuba, Ibaraki 305-0843, Japan. E-mail address: yasutomi@nibio.go.jp

The online version of this article contains supplemental material.

Abbreviations used in this article: BMDC, bone marrow-derived dendritic cell; DC, dendritic cell; dnSOCS1, dominant-negative suppressor of cytokine signaling 1; EAM, experimental autoimmune myocarditis; FS, fractional shortening; KO, knockout; LV, left ventricular; LVEDd, left ventricular end-diastolic dimension; LVESd, left ventricular end-systolic dimension; MyHC-α, cardiac myosin-specific peptide; pdnSOCS1, plasmid vector encoding dominant-negative suppressor of cytokine signaling 1; pSOCS1, plasmid vector encoding suppressor of cytokine signaling 1; QRT-PCR, quantitative real-time RT-PCR; SOCS, suppressor of cytokine signaling.

www.jimmunol.org/cgi/doi/10.4049/jimmunol.1103610

but also innate immunity by suppressing hyperactivation of macrophages and DCs.

In this study, we describe the therapeutic effect of SOCS1 DNA administration using plasmid DNA encoding SOCS1 for EAM. SOCS1 DNA therapy reduces myocarditis by regulating DC populations during EAM.

Materials and Methods

Animals

BALB/c mice and CB17.SCID mice were purchased from CLEA Japan. We used 5–7-wk-old male mice. All animals were cared for according to ethical guidelines approved by the Institutional Animal Care and Use Committee of the National Institute of Biomedical Innovation.

Immunization protocols

Mice were immunized with 100 μg cardiac myosin-specific peptide (MyHC-$\alpha_{614-629}$) Ac-RSLKLMATLFSTYASADR-OH (Toray Research Center) emulsified 1:1 in PBS/CFA (1 mg/ml; H37Ra; Sigma-Aldrich) on days 0 and 7 as described previously (12). For DC immunization, bone marrow-derived DCs (BMDCs) were generated as described (26). BMDCs were pulsed overnight with 10 μg/ml MyHC-α peptide and stimulated for another 4 h with 0.1 μg/ml LPS (Sigma-Aldrich) and 5 μg/ml anti-CD40 (BD Pharmingen) (15). Recipient mice received 2.5×10^5 pulsed and activated BMDCs i.p. on days 0, 2, and 4 and were killed 10 d after the first injection.

Plasmid construction and DNA transfection

Mouse SOCS1 cDNA and dominant-negative SOCS1 (dnSOCS1) cDNA were subcloned into the mammalian vector pcDNA3.1-myc/His(-) using oligonucleotide primers containing restriction sites for XhoI and EchoRI at the 5′ and 3′ ends, respectively. MyHC-α/CFA-immunized mice were injected i.p. with 100 μg of plasmid DNA in 200 μl PBS on days 0, 5, and 10. BMDC-transferred mice and $CD4^+$ T cell adoptive-transferred SCID mice were treated with plasmid DNA on days 0 and 5.

Histopathologic examination

Myocarditis severity was scored on H&E-stained sections using grades from 0–4: 0, no inflammation; 1, <25% of the heart section involved; 2, 25–50%; 3, 50–75%; and 4, >75%. To quantify the fibrotic area, ventricular sections were stained with Sirius Red. The fibrotic area was calculated as the sum of all areas stained positive for Sirius Red divided by the sum of all myocardial areas in each mouse. Two independent researchers scored the slides separately in a blinded manner.

Flow cytometry

Heart inflammatory cells were isolated and processed as described (15, 27). Cells were stained using fluorochrome-conjugated mouse-specific Abs against CD45, CD4, CD3e, CD44, CD62L, and CD40L (BD Biosciences). Samples were analyzed on an FACSCalibur cell sorter (BD Biosciences).

Measurements of cytokines and chemokines

Hearts were homogenized in media containing 2.5% FBS. Supernatants were collected after centrifugation and stored at −80°C. For in vitro stimulation assay of primary $CD4^+$ T cells, naive $CD4^+CD62L^+$ T cells were isolated from the spleens by MACS ($CD4^+CD62L^+$ T Cell Isolation Kit II; Miltenyi Biotec). A total of 1.5×10^7 $CD4^+CD62L^+$ cells were then stimulated with recombinant mouse IL-2 (R&D Systems) or recombinant mouse IL-12 (R&D Systems). Concentrations of cytokines and chemokines in the heart homogenates or culture supernatants were measured with Quantikine ELISA kits (R&D Systems).

Proliferative responses of T cells

Proliferation of T cells was assessed as previously described (28). Briefly, mice were immunized as described above, and the spleens collected on day 14. Cells were cultured with 5 μg/ml MyHC-α for 72 h and pulsed with 0.5 μCi [^{3}H]thymidine 8 h before being measured with a β counter. For in vitro stimulation assay of primary $CD4^+$ T cells, naive $CD4^+CD62L^+$ T cells were isolated from the spleens by MACS ($CD4^+CD62L^+$ T Cell Isolation Kit II; Miltenyi Biotec). A total of 10^5 $CD4^+CD62L^+$ cells were then stimulated with 5 μg/ml anti-CD3ε, 5 μg/ml anti-CD3ε, 1 μg/ml anti-CD28, 50 ng/ml PMA, and 500 ng/ml ionomycin or with 1 μg/ml Con A together with 0.25×10^5 DCs. Proliferative responses were assessed after 48 h in 2.5% RPMI 1640 medium by measurement of the [^{3}H]thymidine incorporation.

Western blot analysis

Total lysates from $CD4^+$ T cells or DCs were immunoblotted and probed with Abs directed against STAT1 (Santa Cruz Biotechnology) and p-STAT1 protein (Cell Signaling Technology). HRP-conjugated goat anti-rabbit IgG (Bio-Rad) was used to identify the binding sites of the primary Ab.

Adoptive transfer of T cells

Splenocytes were collected from diseased mice and cultured with 5 μg/ml MyHC-α for 48 h. A total of 5×10^6 $CD4^+$ T cells were purified by using anti-CD4 magnetic beads (Miltenyi Biotec) and injected i.p. into the SCID mice. The mice were killed 10 d after the injection.

Quantitative real-time RT-PCR

Total RNA was prepared using TRIzol reagent (Invitrogen) according to the manufacturer's instructions. cDNA was synthesized from 1 μg total RNA by reverse transcriptase (Takara). Quantitative real-time RT-PCR (QRT-PCR) analysis was performed with LightCycler (Roche Diagnostics). Primers for mouse *Socs1* were 5′-GTGGTTGTGGAGGGTGAGAT-3′ (sense) and 5′-CCTGAGAGGTGGGATGAGG-3′ (antisense). Primers for mouse *Hprt* were 5′-TCCTCCTCAGACCGCTTTT-3′ (sense) and 5′-CCTGGTTCATCATCGCTAATC-3′ (antisense). Data were normalized by the level of *Hprt* expression in each sample.

Echocardiography

Transthoracic echocardiography was performed on animals on day 35 by using a Prosound α6 with a 10-MHz transducer (Aloka). The left ventricular (LV) chamber dimensions were measured from the M-mode. Two independent investigators who conducted the echocardiography were unaware of the treatment status.

Statistical analysis

All data were expressed as means ± SEM. Statistical analyses were performed using the two-tailed *t* test or Mann–Whitney *U* test for experiments comparing two groups. The *p* values <0.05 were considered statistically significant.

Results

SOCS1 DNA administration inhibits the development of EAM

To examine the effect of in vivo gene delivery of *Socs1* on the pathogenesis of EAM, BALB/c mice were injected with a mammalian expression plasmid vector encoding SOCS1 (pSOCS1) during the course of EAM induction (Fig. 1A). QRT-PCR analysis revealed elevated expression of *Socs1* in the control EAM heart (Fig. 1B). Importantly, in the SOCS1 DNA-administered mice, *Socs1* was strongly expressed in the heart. By day 28, *Socs1* gene expression was significantly elevated in the pSOCS1-treated heart as compared with the controls (Supplemental Fig. 1). Gross cardiac enlargement and edema were reduced in mice with EAM that received pSOCS1 as compared with those in control empty plasmid DNA-administered EAM mice (Fig. 1C). The heart-to-body weight ratio in the pSOCS1-injected mice was significantly decreased as compared with that in the control plasmid-administered mice (Fig. 1D). The pSOCS1-injected EAM mice had a significantly lower myocarditis severity score and fewer infiltrating inflammatory cells than did the control plasmid-injected mice (Fig. 1E–G). The empty vector [pcDNA3.1-myc/His(-)] was used as the control and did not have any effects on EAM in our experiments (data not shown).

Recently, Hanada et al. (29) demonstrated that dnSOCS1, which has a point mutation (F59D) in a functionally critical kinase inhibitory region of SOCS1, strongly augmented cytokine-dependent JAK-STAT activation both in vivo and in vitro as an antagonist of SOCS1. We examined the effect of dnSOCS1 on the clinical course of EAM. Mice administered a plasmid vector

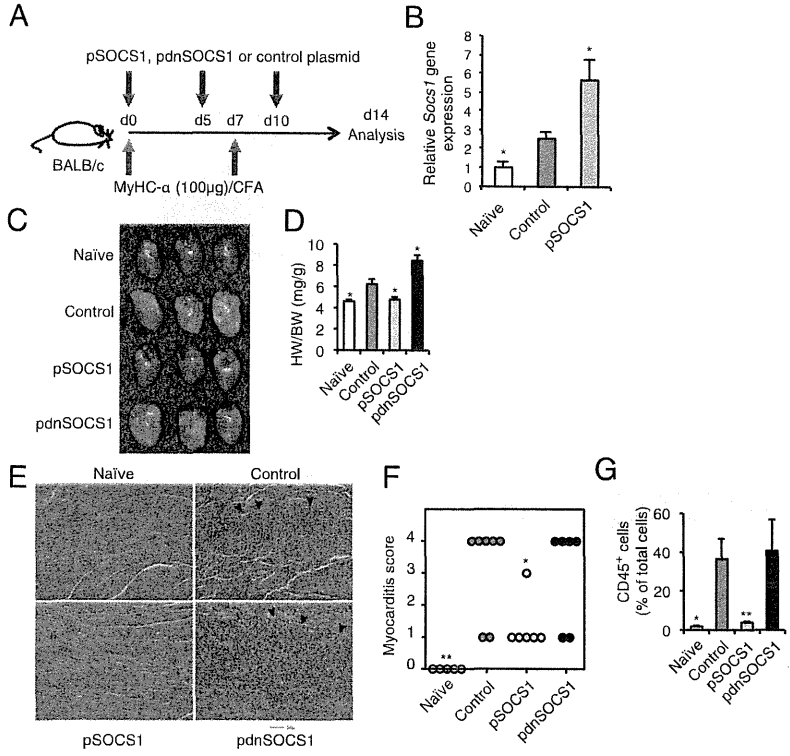

FIGURE 1. Amelioration of EAM and heart failure by SOCS1 DNA administration. (**A**) BALB/c mice were immunized twice, on days 0 and 7, with 100 μg of MyHC-α and treated with pSOCS1, pdnSOCS1, or control plasmid on days 0, 5, and 10. (**B**) QRT-PCR for the *Socs1* gene. RNA samples were obtained from hearts of immunized mice on day 14 and used as a template for QRT-PCR. Results represent the average gene induction in five independent heart samples. (**C**) Representative gross hearts (day 14) of naive and EAM mice treated with the indicated plasmid. (**D**) Heart-to-body weight ratios of naive and EAM mice with indicated treatment (n = 5 mice/group). (**E**) Representative H&E-stained sections of hearts from naive and immunized mice. Arrowheads indicate infiltrating cells. Scale bar, 50 μm. (**F**) Myocarditis severity in heart sections stained with H&E (n = 5–7 mice/group). (**G**) Flow cytometry analysis of $CD45^+$ heart infiltrates of naive and immunized mice (n = 5–7 mice/group). Data are representative of at least two independent experiments. Error bars represent means ± SEM. $*p < 0.05$, $**p < 0.01$ compared with control.

encoding dnSOCS1 (pdnSOCS1) showed augmentation of gross heart enlargement, edema, and heart-to-body weight ratio (Fig. 1C, 1D). However, the myocardial leukocyte infiltration and myocarditis scores were not significantly different between the pdnSOCS1- and control plasmid-administered mice (Fig. 1E–G).

To clarify the adverse effect of dnSOCS1 DNA administration on the development of EAM, we used mice immunized with a tithe amount (10 μg) of MyHC-α instead of the usual amount of peptide for EAM development (Fig. 2A). Those MyHC-α–immunized mice injected with the control plasmid or pSOCS1 did not develop myocarditis (Fig. 2B–F). However, immunized mice injected with pdnSOCS1 developed myocarditis with inflammatory infiltrates (Fig. 2B–F). Thus, administration of pSOCS1 is effective against the development of EAM, and the inhibition of SOCS1 by use of a SOCS1 antagonist adversely affects myocarditis.

SOCS1 DNA administration prevents progression of heart failure and fibrosis after myocarditis

Some patients diagnosed with myocarditis after viral, bacterial, or protozoal infection develop heart failure (2). On day 35 of the present experiment, mice immunized with MyHC-α showed increased LV end-diastolic dimensions (LVEDd) and LV end-systolic dimensions (LVESd) and decreased fractional shortening (FS); however, pSOCS1-injected mice showed almost normal chamber size and LV function (Fig. 3A, 3B). In contrast, LV dysfunction and chamber dilatation in pdnSOCS1-administered mice were manifested as significant increases in LVEDd and LVESd and decrease in FS (Fig. 3A, 3B). In these EAM models, on day 35, hearts from myocarditis mice showed interstitial fibrosis without active leukocyte infiltration. The fibrotic area in mice administered pSOCS1 was significantly smaller than that in control plasmid-injected mice (Fig. 3C, 3D). Although pdnSOCS1-injected mice developed severe cardiac fibrosis, the difference between the fibrotic areas in pdnSOCS1- and control plasmid-injected mice was not statistically significant (Fig. 3C, 3D). These inhibitory effects of pSOCS1 on the development of fibrosis and heart failure were considered to be the result of inhibition of myocardial inflammation because myocarditis developed mice injected with pSOCS1 on day 14, 21, and 28 did not show inhibitory effects on fibrosis and heart failure (data not shown).

Cardiac myosin-specific $CD4^+$ T cell response and cytokine production

Autoimmune myocarditis is a $CD4^+$ T cell-mediated disease (7, 15). Proliferative responses of $CD4^+$ T cells after in vitro restimulation with MyHC-α were not clearly seen in pSOCS1-injected mice; however, the proliferation of $CD4^+$ T cells from pdnSOCS1-injected mice was enhanced (Fig. 4A). Production of IL-2, IL-6, IL-10, IL-17, IL-22, IFN-γ, TNF-α, CCL2, CCL3, CCL5, CCL17, and CXCL10 by $CD4^+$ T cells from EAM mice was enhanced by in vitro restimulation with the MyHC-α epitope peptide. This cardiac-Ag–specific cytokine production by $CD4^+$ T cells was decreased in the supernatants of in vitro MyHC-α–restimulated $CD4^+$ T cells from pSOCS1-administered mice but

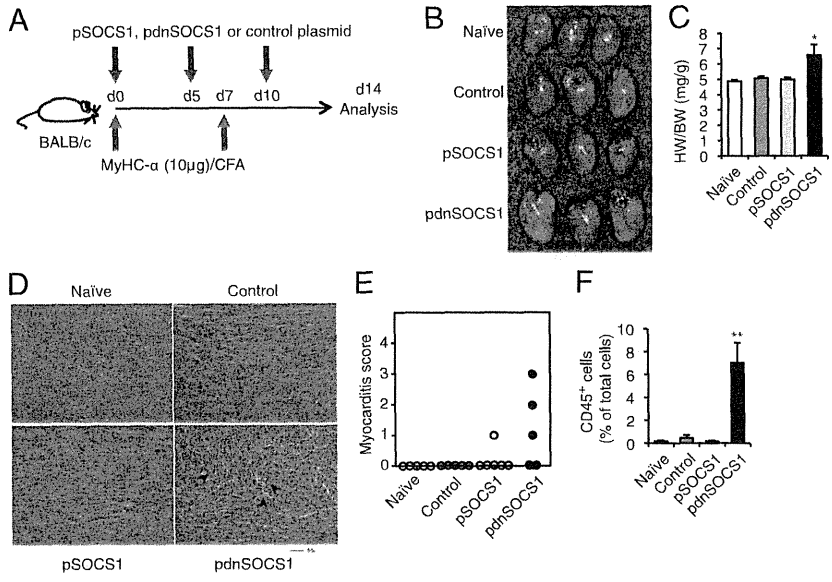

FIGURE 2. Increased susceptibility to EAM induced by inhibition of SOCS1. (**A**) Mice were immunized twice, on days 0 and 7, with 10 μg of MyHC-α emulsified 1:1 in PBS/CFA and treated with pSOCS1, pdnSOCS1, or control plasmid on days 0, 5, and 10. (**B**) Representative gross hearts (day 14) of naive and 10 μg of MyHC-α–immunized mice treated with the indicated plasmid. (**C**) Heart-to-body weight ratios of naive and immunized mice (n = 5 to 6 mice/group). (**D**) Representative H&E-stained sections of hearts from naive and immunized mice. Arrowheads indicate infiltrating cells. Scale bar, 50 μm. (**E**) Myocarditis severity in heart sections stained with H&E (n = 5 to 6 mice/group). (**F**) Flow cytometry analysis of $CD45^+$ heart infiltrates of naive and immunized mice (n = 5 mice/group). Data are representative of at least two independent experiments. Error bars represent means ± SEM. $*p < 0.05$, $**p < 0.01$ compared with control.

was increased in the supernatants of these cells from pdnSOCS1-administered mice (Fig. 4B). In contrast, cardiac-Ag–specific production of IL-1β, IL-10, and CXCL1 was not detected in the culture supernatants of in vitro-restimulated $CD4^+$ T cells from control plasmid-, pSOCS1-, or pdnSOCS1-injected mice (data not shown). Taken together, these results indicate that SOCS1 DNA

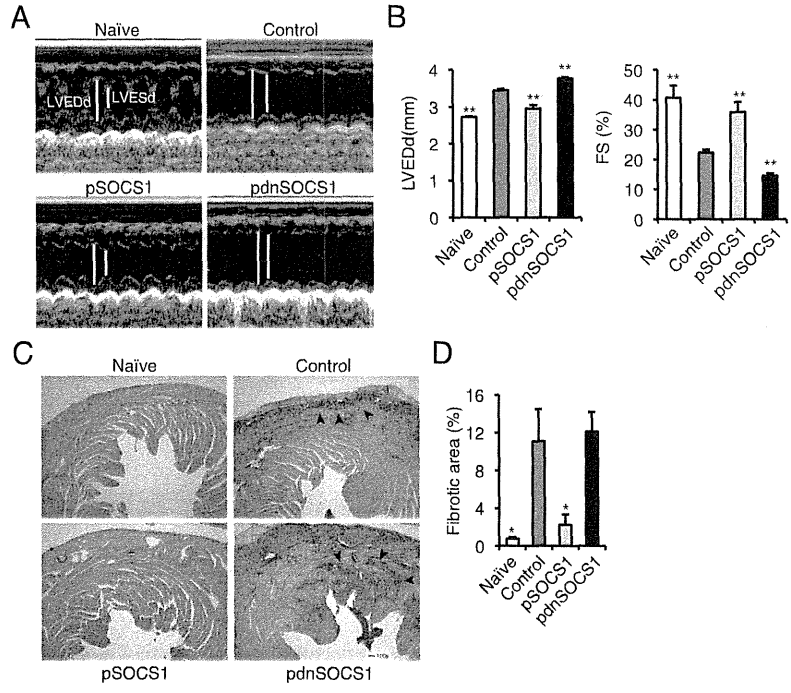

FIGURE 3. SOCS1 DNA administration prevents progression to heart failure. (**A** and **B**) Echocardiography was performed on naive and immunized mice on day 35. (A) Representative M-mode echocardiograms. Bars indicate LVESd and LVEDd. Bar graphs (B) represent LVEDd and percentage of FS from the indicated animals (n = 9 mice/group). The percentage FS was calculated according to the following formula: FS (%) = (LVEDd − LVESd)/LVEDd. (**C** and **D**) Heart tissue sections were stained with Sirius Red and analyzed for fibrosis at day 35. Representative Sirius Red-stained sections of hearts. Scale bar, 50 μm. (C) Arrowheads indicate fibrotic area. (D) The degree of fibrosis was calculated as the percentage of the fibrotic area in relation to the total heart area (n = 5 mice/group). Data are representative of at least two independent experiments. Error bars represent means ± SEM. $*p < 0.05$, $**p < 0.01$ compared with control.

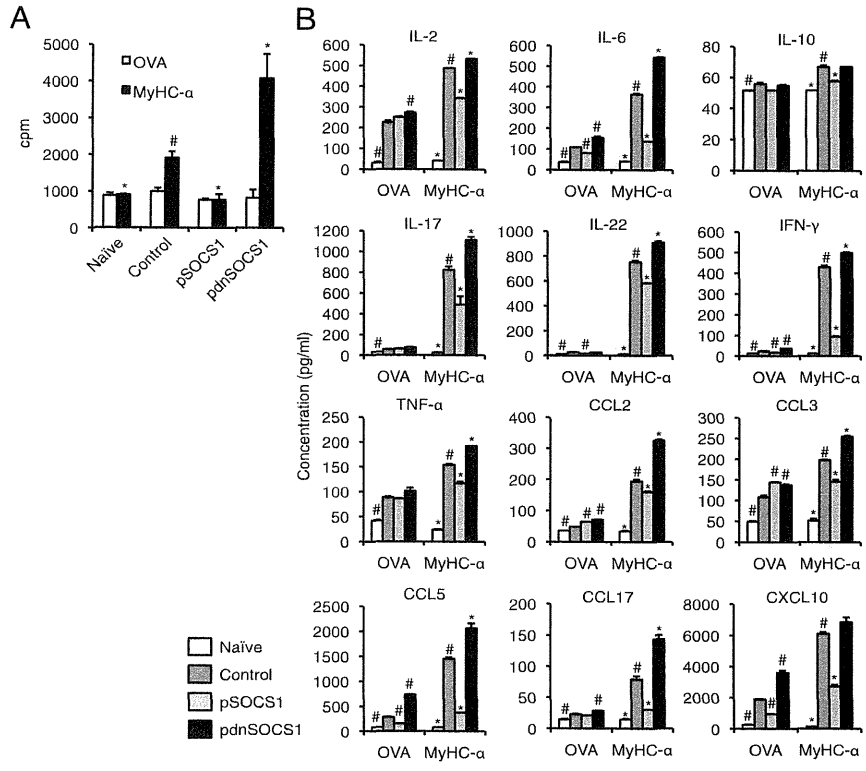

FIGURE 4. Impaired expansion of heart-specific $CD4^+$ T cells in pSOCS1-treated mice. (**A**) Splenocytes were isolated from naive and EAM mice treated with pSOCS1, pdnSOCS1, or control plasmid on day 14 and restimulated in vitro with MyHC-α or OVA peptide for 72 h. Proliferation was assessed by measurement of [^{3}H]thymidine incorporation. Data represent means ± SEM of triplicates from one of three independent experiments. (**B**) Cytokines and chemokines in the culture supernatants of splenocytes were measured by ELISA after 48 h of restimulation with MyHC-α or OVA peptide. Data are expressed as mean ± SEM from triplicate culture wells. Results of one of two representative experiments are shown. $^*p < 0.05$ compared with MyHC-α–stimulated control, $^\#p < 0.05$ compared with OVA-stimulated control.

delivery inhibits the activation of myosin-specific $CD4^+$ T cells and strongly suggest that impaired $CD4^+$ Th cell function prevents EAM development in pSOCS1-injected mice after immunization with cardiac self-Ag.

To evaluate whether pSOCS1 administration affects Ag-specific $CD4^+$ T cell function in other models, we injected plasmid DNA into an autoimmune gastritis model and an OVA-immunized model. In the autoimmune gastritis model, gastric-Ag–specific production of IL-2, IL-6, IL-13, IL-17, IL-22, IFN-γ, TNF-α, CCL2, CCL5, CCL17, and CXCL10 by $CD4^+$ T cells was decreased in pSOCS1-administered mice but increased in pdnSOCS1-administered mice (Supplemental Fig. 2). Lower amounts of cytokines (including IL-2, IL-6, IL-13, IFN-γ, TNF-α, CCL2, CCL3, CCL5, CCL17, and CXCL10) were also produced in $CD4^+$ T cells from pSOCS1-injected OVA-immunized mice (Supplemental Fig. 3). These results suggest that pSOCS1 administration may suppress Ag-specific $CD4^+$ T cell activation in various autoimmune diseases and foreign body infections.

SOCS1 DNA administration inhibits the production of proinflammatory cytokines and $CD4^+$ T cell differentiation in the heart

We also examined whether SOCS1 DNA administration has an effect on cytokine and chemokine milieu in the heart. On day 14 after MyHC-α immunization, heart homogenates from pSOCS1-injected mice had significantly decreased amounts of proinflammatory cytokines, including IL-1β and IL-6, and of myelotropic chemokines, including CCL5, CXCL1, and CXCL10 (Fig. 5A). In contrast, hearts from mice injected with pdnSOCS1 showed greatly increased amounts of proinflammatory cytokines and chemokines (Fig. 5A). SOCS1 protein has been shown to regulate T cell differentiation (17, 18). To determine the differentiation of $CD4^+$ T cells during EAM, we examined the heart-infiltrating $CD4^+$ T cell populations by FACS analysis. Activated $CD4^+$ T cells ($CD4^+CD40L^+$) and effector memory $CD4^+$ T cells ($CD44^+CD62L^-$) were reduced in the pSOCS1-injected mice (Fig. 5B). Thus, protection from EAM in pSOCS1-administered mice is associated with abrogation of proinflammatory cytokines, chemokines, and $CD4^+$ T cell differentiation in the heart.

SOCS1 DNA injection does not have a direct suppressive effect on $CD4^+$ T cell activation

To gain new insights into the mechanism of protection from myocarditis, we investigated whether pSOCS1 therapy directly affects $CD4^+$ T cell activation. Naive T cells ($CD4^+CD62L^+$ cells) were isolated from non-EAM mice injected with pSOCS1, pdnSOCS1, or control plasmid, and their primary responses to various stimuli were compared (Fig. 6A). As shown in Fig. 6B, there were no differences in IFN-γ–induced STAT1 activation among these $CD4^+$ T cells. There were also no differences in primary responses to stimulation with anti-CD3ε, anti-CD3ε/anti-CD28, PMA/ionomycin, or Con A presented by mitomycin C-treated wild-type DCs among pSOCS1-, pdnSOCS1-, and control plasmid-treated $CD4^+$ T cells (Fig. 6C). Chong et al. (30) demonstrated that SOCS1-deficient T cells produced substantially greater levels of IFN-γ in response to IL-2 or IL-12. From these findings, we assessed the production of IFN-γ from $CD4^+$ T cells by using the same experiments. In the culture supernatants of

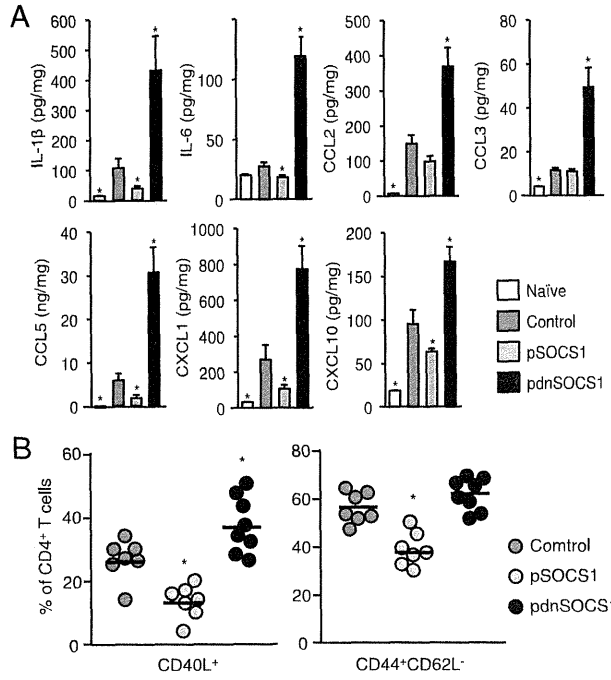

FIGURE 5. Cytokine and chemokine responses and $CD4^+$ T cell differentiation in the heart. (**A**) Myocardial tissues were homogenated and processed by ELISA to detect cytokines and chemokines on day 14. Bar graphs show group means ± SEM of 8–16 mice/group. Results of one of three representative experiments are shown. (**B**) Heart-infiltrating cells were isolated from EAM mice treated with indicated plasmid DNA. Cells were stained for CD4, CD40L, CD44, and CD62L. CD44 and CD62L expression are based on gates set from total $CD4^+$ T cells. Bar graphs show group means ± SEM of 5–9 mice/group. Data are representative of two independent experiments. $*p < 0.05$ compared with control.

$CD4^+$ T cells stimulated with IL-2 or IL-12, there were also no differences in IFN-γ production (Fig. 6D). These results indicate that in vivo administration of pSOCS1 does not directly affect $CD4^+$ T cell activation.

In vivo SOCS1 DNA administration inhibits DC function

Although $CD4^+$ T cell differentiation was inhibited in pSOCS1-treated mice (Fig. 5B), our results suggested that in vivo *Socs1* gene administration has no direct effect on $CD4^+$ T cell activation (Fig. 6). We therefore investigated whether in vivo pSOCS1 administration inhibits the function of Ag-presenting DCs by stimulation through the TLR pathway. DCs from mice administered pSOCS1, pdnSOCS1, or control plasmid were stimulated with LPS for 24 h (Fig. 7A). STAT1 phosphorylation was attenuated in DCs from pSOCS1-injected mice and enhanced in DCs from pdnSOCS1-injected mice (Fig. 7B). The production of proinflammatory cytokines, including IL-6, TNF-α, and IFN-γ, was inhibited in DCs from pSOCS1-injected mice and enhanced in DCs from pdnSOCS1-injected mice (Fig. 7C). These results indicate that in vivo administration of *Socs1* affects DC function. In the current study, the cardiac-Ag–specific proliferative response and cytokine production of $CD4^+$ T cells were inhibited in pSOCS1-injected EAM mice (Fig. 4). We next assessed the functional capability of DCs to prime and expand autoreactive $CD4^+$ T cells from mice injected with each plasmid as a measure of Ag-specific proliferative responses of $CD4^+$ T cells from MyHC-α–immunized mice. Myosin-specific $CD4^+$ T cells were cocultured with MyHC-α–pulsed DCs from pSOCS1-, pdnSOCS1-, and control plasmid-treated mice (Fig. 7D). Interestingly, the proliferative responses of $CD4^+$ T cells cocultured with DCs from pSOCS1-treated mice were much weaker than those of cells cultured with DCs from control plasmid-treated mice, and these proliferative responses of $CD4^+$ T cells were enhanced by coculturing with DCs from pdnSOCS1-administered mice (Fig. 7E). These results suggest that in vivo gene delivery of *Socs1* suppresses the functional capability of DCs to prime and expand autoreactive $CD4^+$ T cells.

SOCS1 DNA administration inhibits the development of myocarditis induced by cardiac myosin peptide-loaded BMDC transfer but not by $CD4^+$ T cell transfer

Functionally interposed SOCS1 is induced in various cell populations, including leukocytes, vascular cells, and cardiomyocytes (18, 31, 32). A mouse model of EAM was established by cell transfer using peptide-pulsed DCs or cardiac epitope-specific $CD4^+$ T cells (7, 14). The effects of pSOCS1 administration in mice transferred with $CD4^+$ T cells from mice with EAM were assessed. pSOCS1, pdnSOCS1, or control plasmid was injected into mice transferred with cardiac myosin-specific $CD4^+$ T cells (Fig. 8A). All mice transferred with $CD4^+$ T cells developed myocarditis, and no therapeutic effects were seen in pSOCS1-injected mice (Fig. 8B–D). Furthermore, pdnSOCS1 administration showed no adverse effect on the status of myocarditis induced by $CD4^+$ T cell transfer (Fig. 8B–D). These findings suggest that systemic injection of pSOCS1 is not effective for inhibition of autoreactive $CD4^+$ T cell activation and recruitment to the heart during myocarditis development. Next, we administered pSOCS1, pdnSOCS1, or control plasmid into mice transferred with MyHC-α–loaded BMDCs (Fig. 8E). Interestingly, pSOCS1 injection inhibited the development of myocarditis after MyHC-α–loaded BMDC transfer, and myocarditis deteriorated after administration of pdnSOCS1 (Fig. 8F–H). These results indicate that the therapeutic effects of SOCS1 DNA administration on EAM contribute to professional APCs such as DCs and also provide evidence for the potential utility of SOCS1 DNA inoculation as an approach to gene therapy for myocarditis.

Discussion

There have been no effective fundamental therapies for acute myocarditis; therefore, supportive care for LV dysfunction is the first line of treatment. Because patients generally present days to weeks after the initial viral infection, antiviral therapy has limited applicability in patients with acute viral myocarditis. The long-term sequelae of viral myocarditis appear to be related to abnormal cellular and humoral immunity; therefore, many clinicians believe that immunosuppression is beneficial for myocarditis treatment (2). In this study, we showed that administration of SOCS1 DNA is effective for inhibiting the development of EAM in BALB/c mice, suggesting a novel immunotherapy for myocarditis. To our knowledge, this is the first report showing that gene delivery of *Socs1* prevents autoimmune disease.

Animal models have greatly advanced our knowledge of the pathogenesis of myocarditis and inflammatory cardiomyopathy. Infection of BALB/c mice with either Coxsackievirus or murine CMV results in the development of acute myocarditis from days 7–14 postinfection that is characterized by myocyte damage due to viral cytotoxicity, and the infectious virus cannot be detected past day 14 of the infection (7). After elimination of viruses, mice showed autoimmune myocarditis, which is associated with mononuclear infiltration of the myocardium and production of autoantibodies to cardiac myosin (7), similar to the pathogenesis of autoimmune myocarditis in humans (3, 4, 33). These autoim-

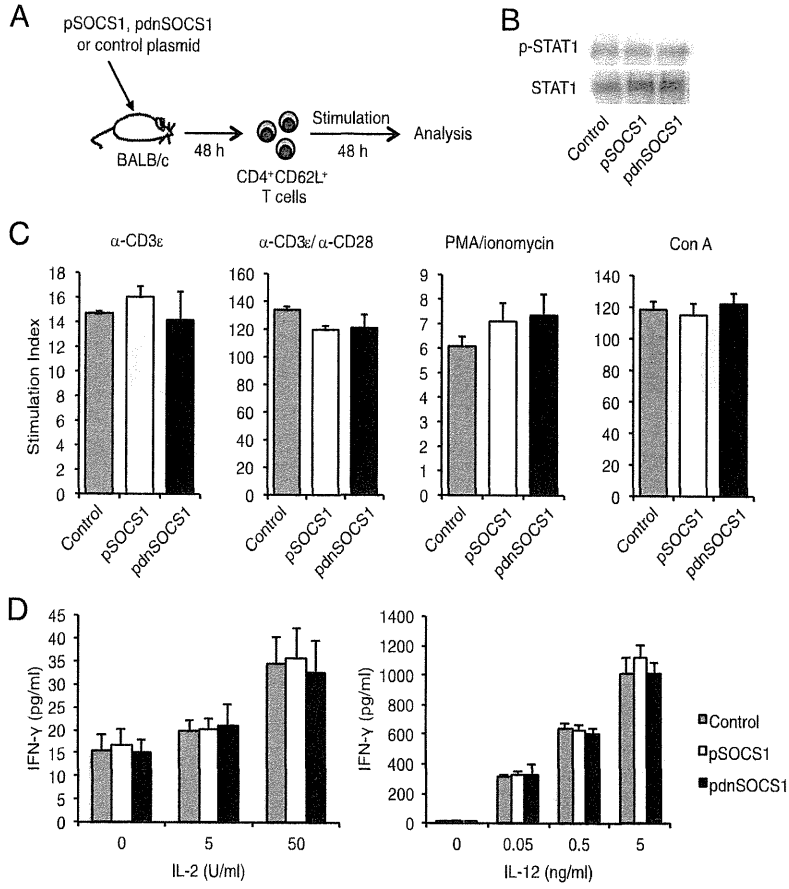

FIGURE 6. Primary responses of $CD4^+$ T cells from pSOCS1-, pdnSOCS1-, and control plasmid-treated mice. (**A**) $CD4^+CD62L^+$ T cells from mice injected with pSOCS1, pdnSOCS1, or control plasmid were stimulated with IFN-γ, anti-CD3ε, anti-CD3ε, anti-CD28, PMA/ionomycin, and Con A in the presence of wild-type DCs, IL-2, or IL-12. (**B**) STAT1 phosphorylation of $CD4^+$ T cells after IFN-γ treatment (10 ng/ml) was assessed by Western blotting. (**C**) T cell proliferation was measured after 48 h of culture. (**D**) IFN-γ in the culture supernatants was measured by ELISA. Values are expressed as means ± SEM of triplicate culture wells. Results of one of at least two representative experiments are shown.

mune responses are thought to be elicited by two mechanisms. One is molecular mimicry: responses to microbial Ags could result in the activation of T cells that are cross-reactive with self-Ags. Another possibility is bystander activation of autoreactive cells. APCs that have become activated in the inflammatory milieu of a pathogenic infection can stimulate the activation and proliferation of autoreactive T or B cells in a process known as bystander activation (reviewed in Ref. 34). Thus, immune responses to myocytes involving various innate and adaptive immune pathways were recognized during myocarditis development. The cardiac myosin peptide-immunized mouse EAM model reflects human autoimmune myocarditis and heart failure after elimination of infectious pathogens.

Recent studies have indicated that various microbes use the host's SOCS proteins for manipulating cytokine receptor signaling as one of the strategies to evade immune responses (35, 36). Coxsackievirus usually infects cardiomyocytes and induces the expression of SOCS1 and SOCS3 in cardiomyocytes, which can result in evasion of immune responses and facilitation of virus replication by inhibition of JAK–STAT signaling (32, 37). These findings indicate that it may be harmful to administer SOCS1 DNA in the acute phase of infectious myocarditis because it may augment viral replication by inhibition of IFN signaling. The effect of SOCS1 transduction on viral myocarditis has been examined by Yasukawa et al. (32). The SOCS1-transgenic mice infected with CVB3 showed increased myocardial injury, virus replication, and mortality. In contrast, they also showed that SOCS1 inhibition in the heart through adeno-associated virus-mediated expression of dnSOCS1 increased resistance to the acute cardiac injury caused by CVB3 infection. These results were acceptable because SOCS proteins have emerged as frequent targets of viral exploitation. Furthermore, when administrating JAK inhibitors, such as SOCS, active serious infections should have been resolved before the start of treatment. It is considered to be inappropriate to use JAK inhibitors for a person with infectious disease or their possibility with consideration for complication of infection (38–40). In contrast, the overactive autoimmune responses triggered by microbial pathogens can persist after elimination of infectious pathogens (7). Therefore, we examined the efficacy of SOCS1 transfection by using EAM induced by cardiac autoantigen immunization in the absence of viral infection. In the current study, we clearly showed the efficacy of *Socs1* gene transfer as an immunosuppressive therapy for myocarditis under infectious pathogen-free conditions in an EAM mice model. The results of a recent randomized, double-blind, placebo-controlled study showed that immunosuppressive therapy, including prednisone and azathioprine, was effective in patients with myocarditis and inflammatory cardiomyopathy and without evidence of the myocardial viral genome (41). These findings indicate that *Socs1* gene transfer can be effective to treat some clinical

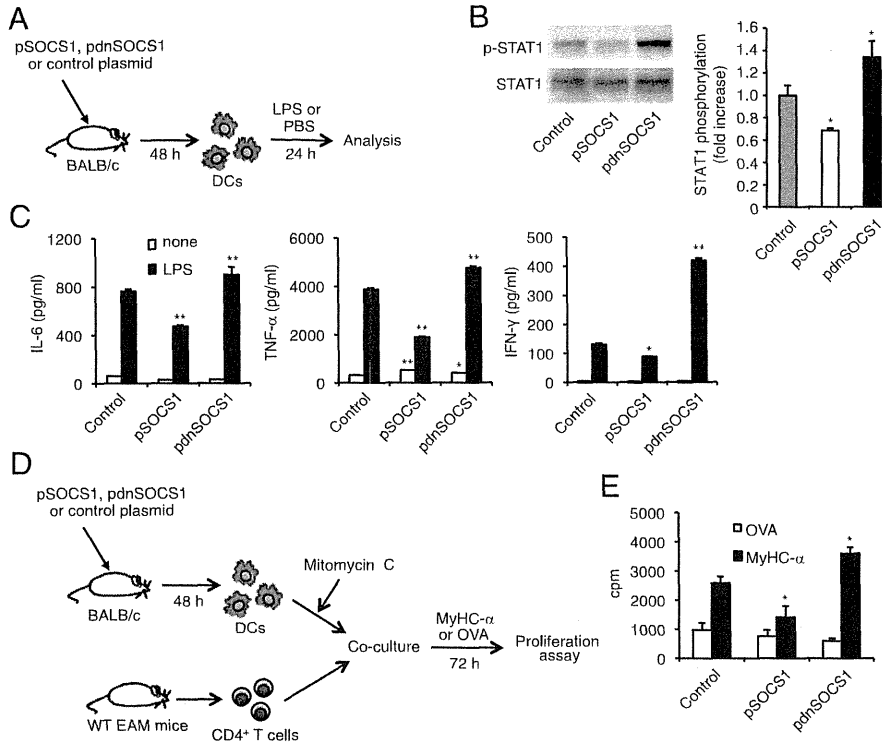

FIGURE 7. Functional capacities of DCs from pSOCS1-, pdnSOCS1-, and control plasmid-treated mice. (**A**) DCs from mice treated with pSOCS1, pdnSOCS1, or control plasmid were stimulated with LPS for 24 h. (**B**) STAT1 phosphorylation of DCs was assessed by Western blotting. Densitometry ratios of pSTAT1/STAT1 are shown as fold induction, the ratio for DCs from control plasmid-injected mice being set at 1. Results are means of five independent experiments ± SEM. Blots are representative of experiments performed a minimum of three times. (**C**) IL-6, TNF-α, and IFN-γ in the culture supernatants were measured by ELISA. Values indicate means ± SEM of triplicate culture wells from one of three independent experiments. (**D** and **E**) Heart-specific $CD4^+$ T cells from EAM mice were restimulated with MyHC-α or OVA peptide on DCs from mice treated with control plasmid, pSOCS1, or pdnSOCS1 for 72 h before measurement of $[^3H]$thymidine incorporation. Each value represents mean ± SEM cpm values of six different culture wells. Results of one of three representative experiments are shown. $^*p < 0.05$, $^{**}p < 0.01$ compared with control.

cases of myocarditis and inflammatory cardiomyopathy associated with autoimmunity and without the virus genome in the myocardium, as well as EAM in mice.

In the current study, we demonstrated that the administration of plasmid DNA encoding SOCS1 did not affect autoreactive $CD4^+$ T cell function (Fig. 6) and adoptive transfer of autoreactive $CD4^+$ T cells was able to induce myocarditis in SOCS1 DNA-administered SCID mice (Fig. 8A–D), suggesting that SOCS1 DNA does not suppress either $CD4^+$ T cell recruitment or accumulation of other inflammatory cells in the heart. In contrast, the introduced SOCS1 DNA inhibited the activation of DCs producing proinflammatory cytokines (Fig. 7C). In fact, inhibition of the phosphorylation of STAT1 molecules was observed in DCs from mice injected with SOCS1 DNA (Fig. 7B). In addition, the proliferative responses of $CD4^+$ T cells cocultured with DCs from pSOCS1-treated mice were much weaker than those of cells cultured with DCs from control plasmid-injected mice (Fig. 7E). These results suggest that the inoculated SOCS1 DNA may have been transfected into DCs and impaired DC function in vivo. Contrary to expectations, we could not find evidence of direct transfection of inoculated DNA into DCs in the heart, spleen, peritoneal cavity, or lymph nodes. Although the introduced DNA is expressed predominantly by somatic cells (e.g., cardiomyocytes, keratinocytes, and fibroblasts), it is known that relatively small but biologically significant numbers of DCs are transfected with the inoculated DNA (42–44). Based on this fact, the inoculated SOCS1 DNA may have inhibited DC activation through the direct transfection into DCs; however, our data do not exclude the possibility of another indirect mechanisms.

In the EAM model, activation of TLRs on self-Ag–presenting DCs is essential for the expansion of autoreactive $CD4^+$ T cells to induce myocarditis and heart failure (15). We previously reported that *Tlr4* mutant C3H/HeJ mice are resistant to development of EAM (45). Furthermore, IL-1 type 1 receptor signaling on DCs is critical for autoimmune myocarditis development (11). MyD88 is a crucial common adaptor molecule that mediates both TLRs and IL-1 type 1 receptor activation (46, 47), and MyD88 signaling in DCs is critical for the induction of EAM (16). SOCS1 negatively regulates the MyD88-dependent pathway by interacting with both IL-1R–associated kinase and NF-κB (17), which results in a decrease in the induction of inflammatory cytokines such as TNF-α and IL-6. In fact, production of these inflammatory cytokines was inhibited by the administration of SOCS1 DNA in the current study (Fig. 7C). Although nearly all TLRs recruit MyD88, other specific adaptor proteins function downstream of particular TLRs. One such adaptor molecule is Toll/IL-1R domain-containing adaptor protein/Mal. SOCS1 also binds to tyrosine-phosphorylated Mal through its interaction with Bruton's tyrosine kinase, leading to the suppression of Mal-dependent p65 phosphorylation and transactivation of NF-κB (48). Another important mechanism of the suppression of APC activation by SOCS1 is inhibition of the secondary activated JAK–STAT pathway (49, 50). The Toll/IL-1R domain-containing adaptor protein-inducing IFN-β–IFN-regulatory factor 3 pathway rapidly induces IFN-β, which in turn activates JAK–STAT1 and contributes to the expression of IFN-

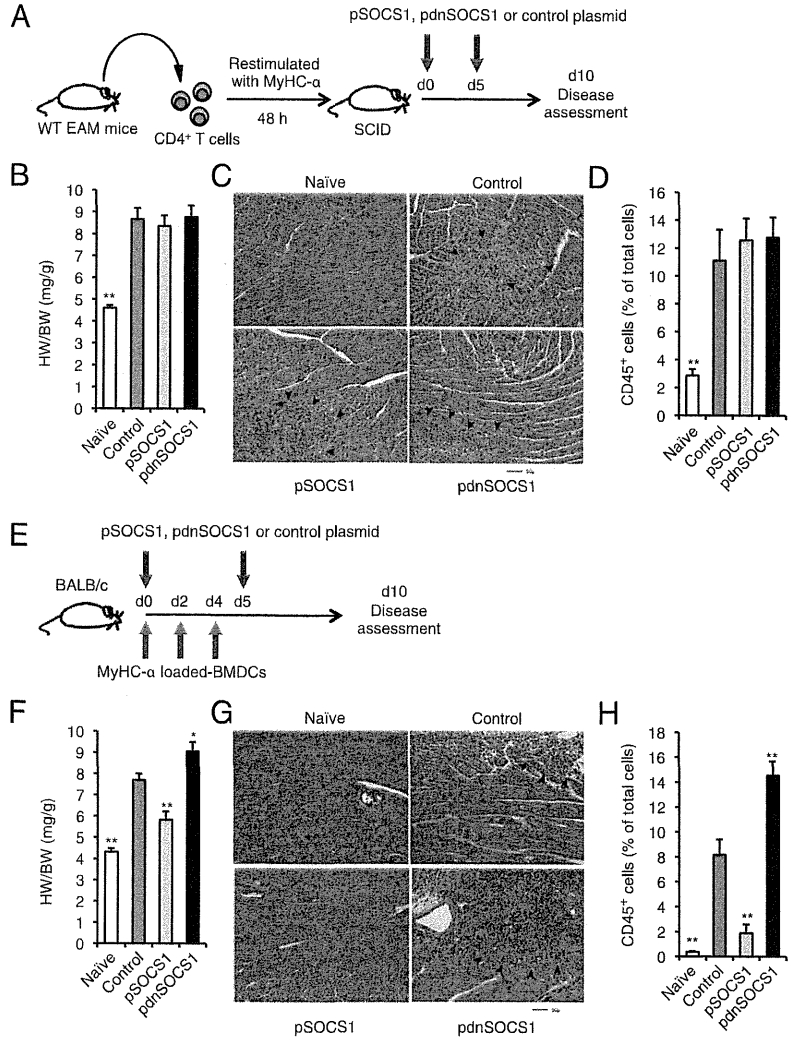

FIGURE 8. pSOCS1 administration inhibited the development of myocarditis induced by cardiac Ag-loaded BMDC injection but not by heart-specific $CD4^+$ T cells. (**A–D**) $CD4^+$ T cells were purified from diseased mice and restimulated in vitro with MyHC-α for 48 h before transfer into SCID recipients. pSOCS1, pdnSOCS1, or control plasmid was injected on days 0 and 5 after the transfer. Heart-to-body weight ratios (B; $n = 5$ mice/group), representative H&E-stained sections of hearts (C), and results of flow cytometry analysis of $CD45^+$ heart infiltrates (D; $n = 5$ mice/group) of naive and adoptive transferred mice at day 10. Arrowheads indicate infiltrating cells. Scale bar, 50 μm. (**E–H**) Mice were immunized with activated MyHC-α– or control OVA peptide-pulsed DCs on days 0, 2, and 4. Mice immunized with MyHC-α–pulsed DCs were treated with pSOCS1, pdnSOCS1, or control plasmid on days 0 and 5. Heart-to-body weight ratios (F; $n = 6$–12 mice/group), representative H&E-stained sections of hearts (G), and results of flow cytometry analysis of $CD45^+$ heart infiltrates (H; $n = 5$ mice/group) of naive and transferred mice at day 10. Arrowheads indicate infiltrating cells. Scale bar, 50 μm. Data are expressed as means ± SEM. Data are representative of at least two independent experiments. $^*p < 0.05$, $^{**}p < 0.01$ compared with control.

inducible genes (51). Moreover, Kimura et al. (52) showed that LPS can activate JAK2 and STAT5, which are involved in IL-6 induction, and that SOCS1 selectively inhibits this process. Thus, SOCS1 negatively regulates several activation pathways in DCs. The present study indicates that pSOCS1 administration is a possible therapy against various diseases caused by overshooting of DCs.

IFN-γ has been shown to be a downregulatory cytokine, as evidenced by exacerbated myocarditis in IFN-γR knockout (KO), IFN-γ KO, and T-bet KO mice (9, 53, 54). In contrast, Th17 cells have recently been implicated in the pathogenesis of various types of autoimmune diseases (reviewed in Ref. 55); however, IL-17 deficiency did not significantly impact the severity of EAM (56). Though these gene-ablated mice provided us with much important information, these studies do not necessarily lead to an effective therapy. In this study, we showed that SOCS1 DNA administration inhibited a broad array of cytokine production from $CD4^+$ T cells (Fig. 4B) and effectively reduced myocardial inflammation (Fig. 1). Compared with inhibition of a single cytokine, SOCS1 DNA therapy could be a more useful therapy that inhibits various signaling pathways to induce production of cytokines.

In the current study, SOCS1 DNA administration was efficacious against EAM development, and inhibition of SOCS1 molecules by SOCS1 antagonist DNA administration enhanced the severity of myocarditis. We demonstrated that SOCS1 DNA administration inhibits the stimulation of self-Ag–presenting DCs inducing cardiac myosin-specific $CD4^+$ T cell responses in peripheral compartments in vivo. Given the availability of clinically effective drugs targeting SOCS1, our findings show new therapeutic perspectives for the treatment of autoimmune myocarditis and cardiomyopathy.

Acknowledgments

We thank T. Okamura, Y. Shiogama, T. Wada, K. Watanabe, H. Shibata, and M. Namikata for technical support and valuable discussion and F. Miyamasu of the Medical English Communications Center, University of Tsukuba, for grammatical revision of this manuscript.

Disclosures

The authors have no financial conflicts of interest.

References

1. Brown, C. A., and J. B. O'Connell. 1995. Myocarditis and idiopathic dilated cardiomyopathy. *Am. J. Med.* 99: 309–314.
2. Feldman, A. M., and D. McNamara. 2000. Myocarditis. *N. Engl. J. Med.* 343: 1388–1398.
3. Caforio, A. L., N. J. Mahon, F. Tona, and W. J. McKenna. 2002. Circulating cardiac autoantibodies in dilated cardiomyopathy and myocarditis: pathogenetic and clinical significance. *Eur. J. Heart Fail.* 4: 411–417.
4. Lauer, B., M. Schannwell, U. Kühl, B. E. Strauer, and H. P. Schultheiss. 2000. Antimyosin autoantibodies are associated with deterioration of systolic and diastolic left ventricular function in patients with chronic myocarditis. *J. Am. Coll. Cardiol.* 35: 11–18.
5. Frustaci, A., C. Chimenti, F. Calabrese, M. Pieroni, G. Thiene, and A. Maseri. 2003. Immunosuppressive therapy for active lymphocytic myocarditis: virological and immunologic profile of responders versus nonresponders. *Circulation* 107: 857–863.
6. Caforio, A. L., J. H. Goldman, A. J. Haven, K. M. Baig, L. D. Libera, and W. J. McKenna; The Myocarditis Treatment Trial Investigators. 1997. Circulating cardiac-specific autoantibodies as markers of autoimmunity in clinical and biopsy-proven myocarditis. *Eur. Heart J.* 18: 270–275.
7. Fairweather, D., Z. Kaya, G. R. Shellam, C. M. Lawson, and N. R. Rose. 2001. From infection to autoimmunity. *J. Autoimmun.* 16: 175–186.
8. Eriksson, U., M. O. Kurrer, W. Sebald, F. Brombacher, and M. Kopf. 2001. Dual role of the IL-12/IFN-gamma axis in the development of autoimmune myocarditis: induction by IL-12 and protection by IFN-gamma. *J. Immunol.* 167: 5464–5469.
9. Afanasyeva, M., Y. Wang, Z. Kaya, E. A. Stafford, K. M. Dohmen, A. A. Sadighi Akha, and N. R. Rose. 2001. Interleukin-12 receptor/STAT4 signaling is required for the development of autoimmune myocarditis in mice by an interferon-gamma-independent pathway. *Circulation* 104: 3145–3151.
10. Eriksson, U., M. O. Kurrer, N. Schmitz, S. C. Marsch, A. Fontana, H. P. Eugster, and M. Kopf. 2003. Interleukin-6-deficient mice resist development of autoimmune myocarditis associated with impaired upregulation of complement C3. *Circulation* 107: 320–325.
11. Eriksson, U., M. O. Kurrer, I. Sonderegger, G. Iezzi, A. Tafuri, L. Hunziker, S. Suzuki, K. Bachmaier, R. M. Bingisser, J. M. Penninger, and M. Kopf. 2003. Activation of dendritic cells through the interleukin 1 receptor 1 is critical for the induction of autoimmune myocarditis. *J. Exp. Med.* 197: 323–331.
12. Sonderegger, I., G. Iezzi, R. Maier, N. Schmitz, M. Kurrer, and M. Kopf. 2008. GM-CSF mediates autoimmunity by enhancing IL-6-dependent Th17 cell development and survival. *J. Exp. Med.* 205: 2281–2294.
13. Satoh, M., G. Tamura, I. Segawa, A. Tashiro, K. Hiramori, and R. Satodate. 1996. Expression of cytokine genes and presence of enteroviral genomic RNA in endomyocardial biopsy tissues of myocarditis and dilated cardiomyopathy. *Virchows Arch.* 427: 503–509.
14. Eriksson, U., and J. M. Penninger. 2005. Autoimmune heart failure: new understandings of pathogenesis. *Int. J. Biochem. Cell Biol.* 37: 27–32.
15. Eriksson, U., R. Ricci, L. Hunziker, M. O. Kurrer, G. Y. Oudit, T. H. Watts, I. Sonderegger, K. Bachmaier, M. Kopf, and J. M. Penninger. 2003. Dendritic cell-induced autoimmune heart failure requires cooperation between adaptive and innate immunity. *Nat. Med.* 9: 1484–1490.
16. Marty, R. R., S. Dirnhofer, N. Maucrmann, S. Schweikert, S. Akira, L. Hunziker, J. M. Penninger, and U. Eriksson. 2006. MyD88 signaling controls autoimmune myocarditis induction. *Circulation* 113: 258–265.
17. Dimitriou, I. D., L. Clemenza, A. J. Scotter, G. Chen, F. M. Guerra, and R. Rottapel. 2008. Putting out the fire: coordinated suppression of the innate and adaptive immune systems by SOCS1 and SOCS3 proteins. *Immunol. Rev.* 224: 265–283.
18. Yoshimura, A., T. Naka, and M. Kubo. 2007. SOCS proteins, cytokine signalling and immune regulation. *Nat. Rev. Immunol.* 7: 454–465.
19. Shuai, K., and B. Liu. 2003. Regulation of JAK-STAT signalling in the immune system. *Nat. Rev. Immunol.* 3: 900–911.
20. Croker, B. A., H. Kiu, and S. E. Nicholson. 2008. SOCS regulation of the JAK/STAT signalling pathway. *Semin. Cell Dev. Biol.* 19: 414–422.
21. Fujimoto, M., and T. Naka. 2010. SOCS1, a Negative Regulator of Cytokine Signals and TLR Responses, in Human Liver Diseases. *Gastroenterol. Res. Pract.* 2010: 2010.
22. Naka, T., M. Fujimoto, H. Tsutsui, and A. Yoshimura. 2005. Negative regulation of cytokine and TLR signalings by SOCS and others. *Adv. Immunol.* 87: 61–122.
23. Hanada, T., H. Yoshida, S. Kato, K. Tanaka, K. Masutani, J. Tsukada, Y. Nomura, H. Mimata, M. Kubo, and A. Yoshimura. 2003. Suppressor of cytokine signaling-1 is essential for suppressing dendritic cell activation and systemic autoimmunity. *Immunity* 19: 437–450.
24. Kinjyo, I., T. Hanada, K. Inagaki-Ohara, H. Mori, D. Aki, M. Ohishi, H. Yoshida, M. Kubo, and A. Yoshimura. 2002. SOCS1/JAB is a negative regulator of LPS-induced macrophage activation. *Immunity* 17: 583–591.
25. Nakagawa, R., T. Naka, H. Tsutsui, M. Fujimoto, A. Kimura, T. Abe, E. Seki, S. Sato, O. Takeuchi, K. Takeda, et al. 2002. SOCS-1 participates in negative regulation of LPS responses. *Immunity* 17: 677–687.
26. Lutz, M. B., N. Kukutsch, A. L. Ogilvie, S. Rössner, F. Koch, N. Romani, and G. Schuler. 1999. An advanced culture method for generating large quantities of highly pure dendritic cells from mouse bone marrow. *J. Immunol. Methods* 223: 77–92.
27. Valaperti, A., R. R. Marty, G. Kania, D. Germano, N. Mauermann, S. Dirnhofer, B. Leimenstoll, P. Blyszczuk, C. Dong, C. Mueller, et al. 2008. CD11b+ monocytes abrogate Th17 CD4+ T cell-mediated experimental autoimmune myocarditis. *J. Immunol.* 180: 2686–2695.
28. Cihakova, D., J. G. Barin, M. Afanasyeva, M. Kimura, D. Fairweather, M. Berg, M. V. Talor, G. C. Baldeviano, S. Frisancho, K. Gabrielson, et al. 2008. Interleukin-13 protects against experimental autoimmune myocarditis by regulating macrophage differentiation. *Am. J. Pathol.* 172: 1195–1208.
29. Hanada, T., T. Yoshida, I. Kinjyo, S. Minoguchi, H. Yasukawa, S. Kato, H. Mimata, Y. Nomura, Y. Seki, M. Kubo, and A. Yoshimura. 2001. A mutant form of JAB/SOCS1 augments the cytokine-induced JAK/STAT pathway by accelerating degradation of wild-type JAB/CIS family proteins through the SOCS-box. *J. Biol. Chem.* 276: 40746–40754.
30. Chong, M. M., D. Metcalf, E. Jamieson, W. S. Alexander, and T. W. Kay. 2005. Suppressor of cytokine signaling-1 in T cells and macrophages is critical for preventing lethal inflammation. *Blood* 106: 1668–1675.
31. Ortiz-Muñoz, G., J. L. Martin-Ventura, P. Hernandez-Vargas, B. Mallavia, V. Lopez-Parra, O. Lopez-Franco, B. Muñoz-Garcia, P. Fernandez-Vizarra, L. Ortega, J. Egido, and C. Gomez-Guerrero. 2009. Suppressors of cytokine signaling modulate JAK/STAT-mediated cell responses during atherosclerosis. *Arterioscler. Thromb. Vasc. Biol.* 29: 525–531.
32. Yasukawa, H., T. Yajima, H. Duplain, M. Iwatate, M. Kido, M. Hoshijima, M. D. Weitzman, T. Nakamura, S. Woodard, D. Xiong, et al. 2003. The suppressor of cytokine signaling-1 (SOCS1) is a novel therapeutic target for enterovirus-induced cardiac injury. *J. Clin. Invest.* 111: 469–478.
33. Kanzaki, Y., F. Terasaki, M. Okabe, T. Hayashi, H. Toko, H. Shimomura, S. Fujioka, Y. Kitaura, K. Kawamura, Y. Horii, et al. 2001. Myocardial inflammatory cell infiltrates in cases of dilated cardiomyopathy as a determinant of outcome following partial left ventriculectomy. *Jpn. Circ. J.* 65: 797–802.
34. Münz, C., J. D. Lünemann, M. T. Getts, and S. D. Miller. 2009. Antiviral immune responses: triggers of or triggered by autoimmunity? *Nat. Rev. Immunol.* 9: 246–258.
35. Baetz, A., S. Zimmermann, and A. H. Dalpke. 2007. Microbial immune evasion employing suppressor of cytokine signaling (SOCS) proteins. *Inflamm. Allergy Drug Targets* 6: 160–167.
36. Akhtar, L. N., and E. N. Benveniste. 2011. Viral exploitation of host SOCS protein functions. *J. Virol.* 85: 1912–1921.
37. Yajima, T., H. Yasukawa, E. S. Jeon, D. Xiong, A. Dorner, M. Iwatate, M. Nara, H. Zhou, D. Summers-Torres, M. Hoshijima, et al. 2006. Innate defense mechanism against virus infection within the cardiac myocyte requiring gp130-STAT3 signaling. *Circulation* 114: 2364–2373.
38. Pesu, M., A. Laurence, N. Kishore, S. H. Zwillich, G. Chan, and J. J. O'Shea. 2008. Therapeutic targeting of Janus kinases. *Immunol. Rev.* 223: 132–142.
39. Yamaoka, K., B. Min, Y. J. Zhou, W. E. Paul, and J. J. O'shea. 2005. Jak3 negatively regulates dendritic-cell cytokine production and survival. *Blood* 106: 3227–3233.
40. Changelian, P. S., D. Moshinsky, C. F. Kuhn, M. E. Flanagan, M. J. Munchhof, T. M. Harris, D. A. Whipple, J. L. Doty, J. Sun, C. R. Kent, et al. 2008. The specificity of JAK3 kinase inhibitors. *Blood* 111: 2155–2157.
41. Frustaci, A., M. A. Russo, and C. Chimenti. 2009. Randomized study on the efficacy of immunosuppressive therapy in patients with virus-negative inflammatory cardiomyopathy: the TIMIC study. *Eur. Heart J.* 30: 1995–2002.
42. Tüting, T., W. J. Storkus, and L. D. Falo, Jr. 1998. DNA immunization targeting the skin: molecular control of adaptive immunity. *J. Invest. Dermatol.* 111: 183–188.
43. Condon, C., S. C. Watkins, C. M. Celluzzi, K. Thompson, and L. D. Falo, Jr. 1996. DNA-based immunization by in vivo transfection of dendritic cells. *Nat. Med.* 2: 1122–1128.
44. Porgador, A., K. R. Irvine, A. Iwasaki, B. H. Barber, N. P. Restifo, and R. N. Germain. 1998. Predominant role for directly transfected dendritic cells in antigen presentation to CD8+ T cells after gene gun immunization. *J. Exp. Med.* 188: 1075–1082.
45. Nishikubo, K., K. Imanaka-Yoshida, S. Tamaki, M. Hiroe, T. Yoshida, Y. Adachi, and Y. Yasutomi. 2007. Th1-type immune responses by Toll-like receptor 4 signaling are required for the development of myocarditis in mice with BCG-induced myocarditis. *J. Autoimmun.* 29: 146–153.
46. Akira, S., and H. Hemmi. 2003. Recognition of pathogen-associated molecular patterns by TLR family. *Immunol. Lett.* 85: 85–95.
47. Li, X., and J. Qin. 2005. Modulation of Toll-interleukin 1 receptor mediated signaling. *J. Mol. Med.* 83: 258–266.
48. Mansell, A., R. Smith, S. L. Doyle, P. Gray, J. E. Fenner, P. J. Crack, S. E. Nicholson, D. J. Hilton, L. A. O'Neill, and P. J. Hertzog. 2006. Suppressor of cytokine signaling 1 negatively regulates Toll-like receptor signaling by mediating Mal degradation. *Nat. Immunol.* 7: 148–155.
49. Gingras, S., E. Parganas, A. de Pauw, J. N. Ihle, and P. J. Murray. 2004. Re-examination of the role of suppressor of cytokine signaling 1 (SOCS1) in the regulation of toll-like receptor signaling. *J. Biol. Chem.* 279: 54702–54707.
50. Baetz, A., M. Frey, K. Heeg, and A. H. Dalpke. 2004. Suppressor of cytokine signaling (SOCS) proteins indirectly regulate toll-like receptor signaling in innate immune cells. *J. Biol. Chem.* 279: 54708–54715.

51. Qin, H., C. A. Wilson, S. J. Lee, and E. N. Benveniste. 2006. IFN-beta-induced SOCS-1 negatively regulates CD40 gene expression in macrophages and microglia. *FASEB J.* 20: 985–987.
52. Kimura, A., T. Naka, T. Muta, O. Takeuchi, S. Akira, I. Kawase, and T. Kishimoto. 2005. Suppressor of cytokine signaling-1 selectively inhibits LPS-induced IL-6 production by regulating JAK-STAT. *Proc. Natl. Acad. Sci. USA* 102: 17089–17094.
53. Eriksson, U., M. O. Kurrer, R. Bingisser, H. P. Eugster, P. Saremaslani, F. Follath, S. Marsch, and U. Widmer. 2001. Lethal autoimmune myocarditis in interferon-gamma receptor-deficient mice: enhanced disease severity by impaired inducible nitric oxide synthase induction. *Circulation* 103: 18–21.
54. Rangachari, M., N. Mauermann, R. R. Marty, S. Dirnhofer, M. O. Kurrer, V. Komnenovic, J. M. Penninger, and U. Eriksson. 2006. T-bet negatively regulates autoimmune myocarditis by suppressing local production of interleukin 17. *J. Exp. Med.* 203: 2009–2019.
55. Ghoreschi, K., A. Laurence, X. P. Yang, K. Hirahara, and J. J. O'Shea. 2011. T helper 17 cell heterogeneity and pathogenicity in autoimmune disease. *Trends Immunol.* 32: 395–401.
56. Baldeviano, G. C., J. G. Barin, M. V. Talor, S. Srinivasan, D. Bedja, D. Zheng, K. Gabrielson, Y. Iwakura, N. R. Rose, and D. Cihakova. 2010. Interleukin-17A is dispensable for myocarditis but essential for the progression to dilated cardiomyopathy. *Circ. Res.* 106: 1646–1655.

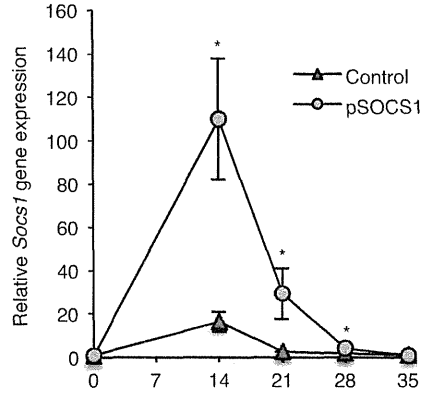

Supplementary Figure 1. *Socs1* gene expression in the heart. RNA samples were obtained from EAM hearts on days 0, 14, 21, 28 and 35, and used as a template for QRT-PCR. Results represent the average gene induction in five to six independent heart samples. Results of one of two representative experiments are shown. $*P < 0.05$ compared to control.

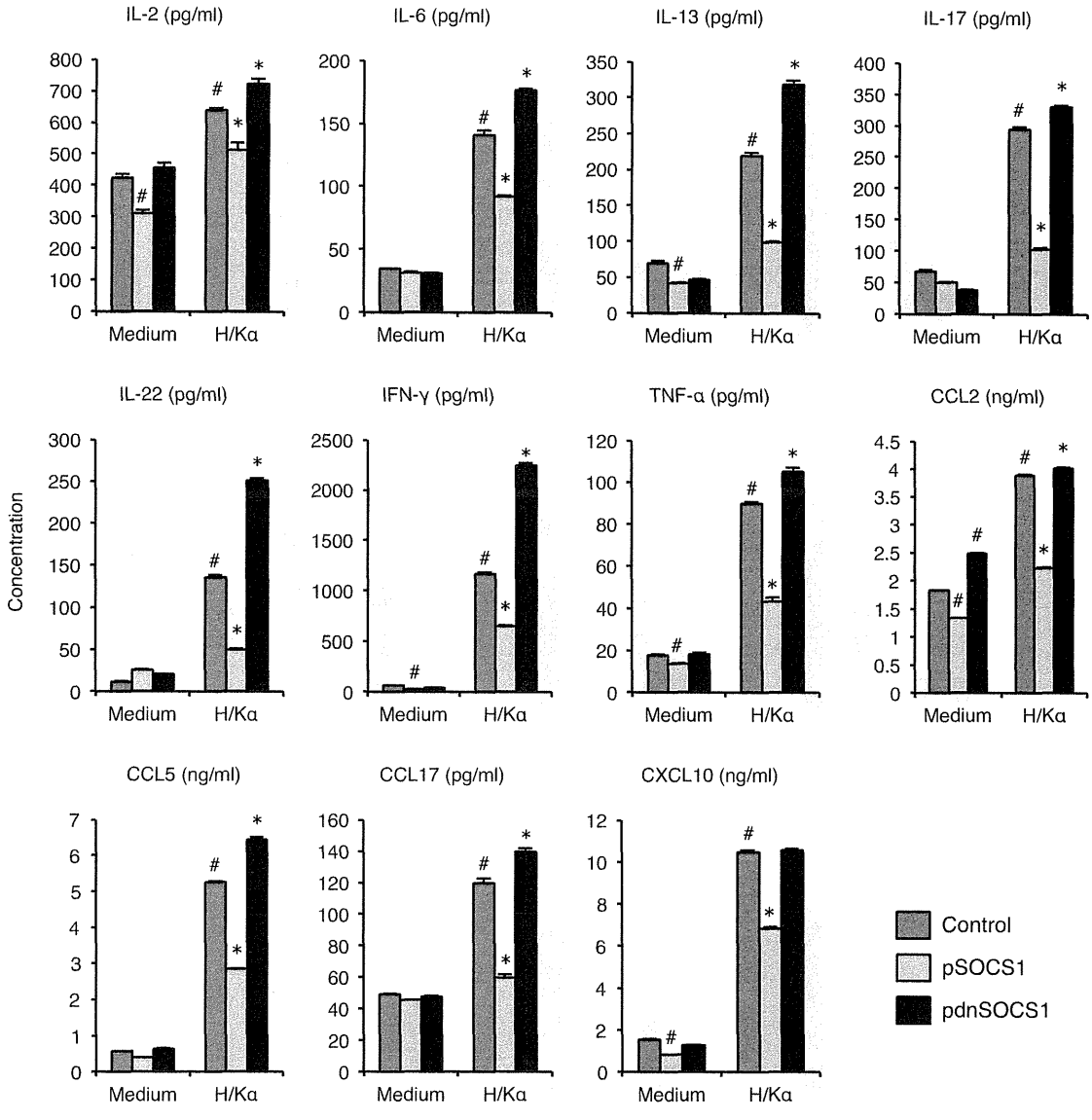

Supplementary Figure 2. Impaired cytokine production by H^+/K^+ ATPase α (H/Kα)-specific $CD4^+$ T cells in pSOCS1-treated mice. BALB/c mice were immunized twice, on days 0 and 7, with 100 μg of H/Kα p253-277 in an emulsion with CFA and treated with pSOCS1, pdnSOCS1 or control plasmid on days 0, 5 and 10. Splenocytes were isolated from mice on day 14 and cultured in the absence or presence of H/Kα peptide (1 μg/ml) for 72 h. Cytokines and chemokines in the culture supernatants were measured by ELISA. Data are expressed as mean ± SEM from triplicate culture wells. Results of one of two representative experiments are shown. *$P < 0.05$ compared to H/Kα stimulated control and #$P < 0.05$ compared to unstimulated control.

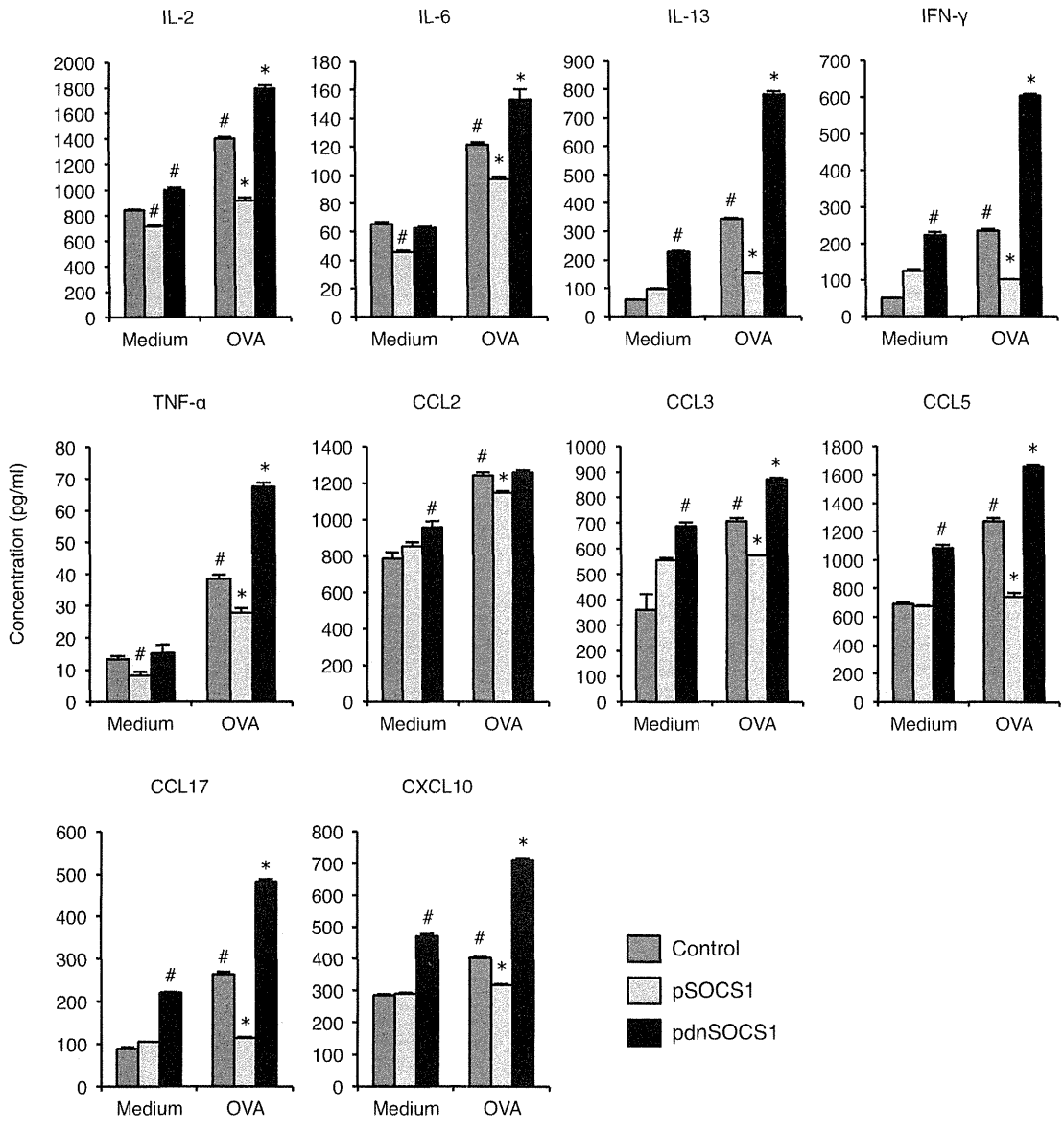

Supplementary Figure 3. Impaired cytokine production by OVA-specific CD4$^+$ T cells in pSOCS1-treated mice. BALB/c mice were immunized twice, on days 0 and 7, with 100 μg of OVA p323-339 in an emulsion with alum and treated with pSOCS1, pdnSOCS1 or control plasmid on days 0, 5 and 10. Splenocytes were isolated from mice on day 14 and cultured in the absence or presence of OVA peptide (5 μg/ml) for 72 h. Cytokines and chemokines in the culture supernatants were measured by ELISA. Data are expressed as mean ± SEM from triplicate culture wells. Results of one of two representative experiments are shown. *$P < 0.05$ compared to OVA stimulated control and #$P < 0.05$ compared to unstimulated control.

Focus Article

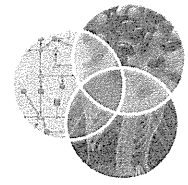

Systems biology approaches to toll-like receptor signaling

Alexis Vandenbon,[1†] Shunsuke Teraguchi,[2†] Shizuo Akira,[2,5] Kiyoshi Takeda[3,4] and Daron M. Standley[1*]

Toll-like receptor (TLR) signaling pathways constitute an evolutionarily conserved host defense system that protects against a broad range of infectious agents. Modeling of TLR signaling has been carried out at several levels. Structural models of TLRs and their adaptors, which utilize a small number of structural domains to recognize a diverse range of pathogens, provide a starting point for understanding how pathogens are recognized and signaling events initiated. Various experimental and computational techniques have been used to construct models of downstream signal transduction networks from the measurements of gene expression and chromatin structure under resting and perturbed conditions along with predicted regulatory sequence motifs. Although a complete and accurate mathematical model of all TLR signaling pathways has yet to be derived, many important modules have been identified and investigated, enhancing our understanding of innate immune responses. Extensions of these models based on emerging experimental techniques are discussed.

How to cite this article:
WIREs Syst Biol Med 2012, 4:497–507. doi: 10.1002/wsbm.1178

INTRODUCTION

Pattern recognition receptors (PRRs) that specifically bind to evolutionarily conserved pathogen-associated molecular patterns (PAMPs) play a key role in host defense. Of the PRRs, the toll-like receptors (TLRs) are the best characterized, both in terms of the PAMPs they recognize and the corresponding pathways that are activated in response to their binding. To date, 10 TLRs have been identified in humans, each of which has a homolog in mouse. Identifying the ligand specificity and downstream pathways of each TLR (or combination, as TLRs function as dimers) has been the subject of intense research for the last 15 years.[1,2] Two main TLR signaling pathways have been identified: the MyD88 (myeloid differentiation factor 88)-dependent[3] and the TRIF (TIR-domain-containing adaptor protein-inducing IFN-β)-dependent[4] pathways. The MyD88-dependent pathway is activated by all known TLRs except TLR3, and leads to the production of proinflammatory cytokines. TLR3 and TLR4 can activate the TRIF-dependent pathway, which leads to the production of type I interferons (IFNs) against viral infection. Hundreds of proteins have been characterized as players in the innate immune response, and thousands of genes whose expression levels change upon TLR stimulation have been identified. Many protein–protein interactions have been determined for TLR signaling molecules as well.[5] However, a successful immune response requires the coordinated interaction between all of its parts, from a molecular to an intercellular level. Reconstructing and reproducing this system-level behavior are a daunting task, and one that is impossible to accomplish without the development of multilevel and multi-timescale computational frameworks. In this review we will summarize

†These authors contributed equally to this work.

*Correspondence to: standley@ifrec.osaka-u.ac.jp

[1]Laboratory of Systems Immunology, WPI Immunology Frontier Research Center (IFReC), Osaka University, Suita, Osaka, Japan

[2]Laboratory of Host Defence, WPI Immunology Frontier Research Center (IFReC), Osaka University, Suita, Osaka, Japan

[3]Department of Microbiology and Immunology, Graduate School of Medicine, Osaka University, Suita, Osaka, Japan

[4]Laboratory of Mucosal Immunology, WPI Immunology Frontier Research Center (IFReC) Osaka University, Suita, Osaka, Japan

[5]Research Institute for Microbial Diseases, Osaka University, Suita, Osaka, Japan

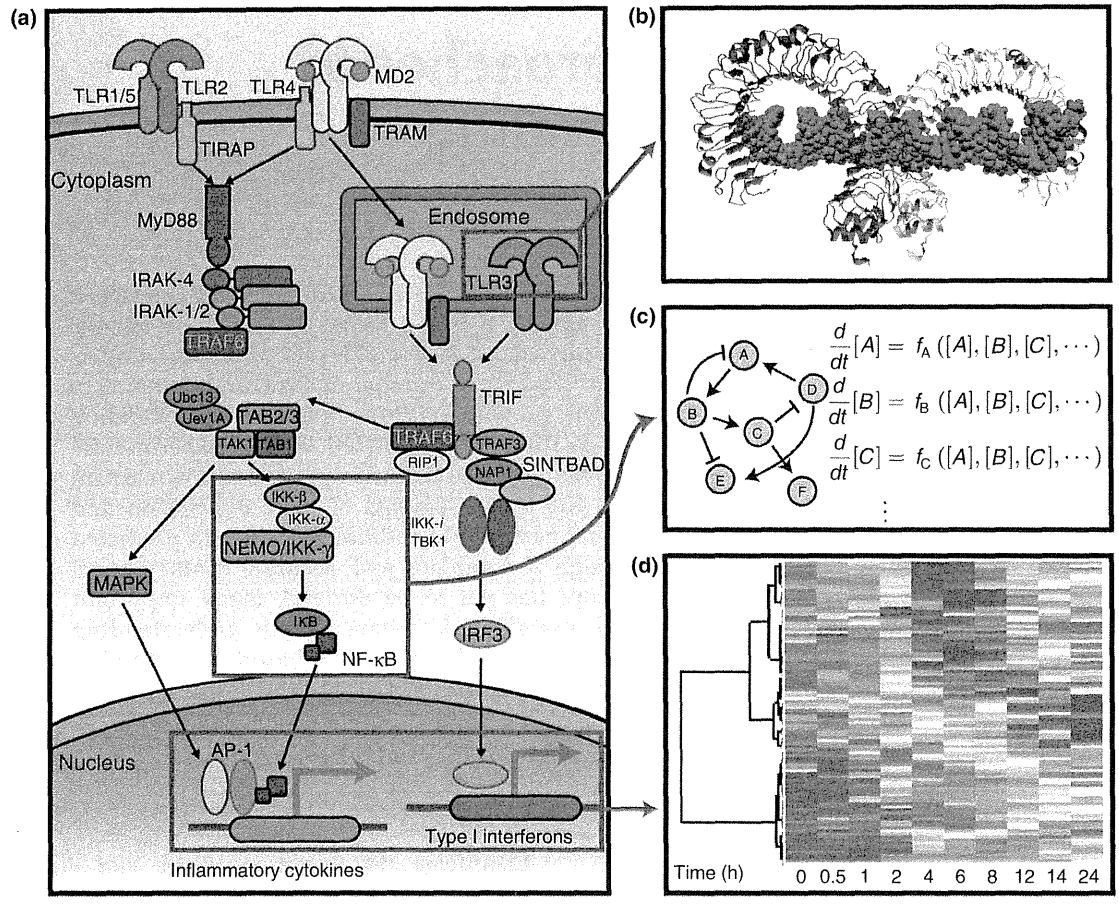

FIGURE 1 | Multi-scale modeling of toll-like receptor (TLR) pathways. (a) The MyD88- and TRIF-dependent pathways are illustrated. Reprinted with permission from Ref 2 Copyright 2010 Elsevier. (b) The X-ray structure of TLR3 leucine rich repeat (LRR) domains bound to double-stranded RNA. (c) A mathematical model of a hypothetical signaling network between components A–F. (d) A heatmap of gene expression values at 10 time points.

the current models, focusing on structure, signal transduction, and gene expression analysis (Figure 1).

STRUCTURAL MODELING OF TLRs AND THEIR ADAPTORS

Homology modeling (Box 1) has played an important role in the analysis of TLR signaling pathways because a number of structural domains reoccur in various contexts. As shown in Figure 2, each of the TLRs contains an N-terminal leucine rich repeat (LRR) domain, followed by a transmembrane helix and a cytoplasmic C-terminal toll/interleukin-1 receptor (TIR) domain. The cytoplasmic TIR domains, in turn, bind TIR-containing adapter molecules. In the case of the MyD88-dependent TLR4 signaling pathway, for example, a TLR4 TIR domain homodimer interacts directly with the TIR-containing adaptor TIRAP (TIR-associated protein; also known as Mal).[6,7] TIRAP, in turn, interacts directly with MyD88,[8] which contains both a TIR domain and a death domain (DD). The MyD88 DD interacts with DD-containing IL-1R-associated kinase-4 (IRAK-4), which interacts with DD-containing IRAK-2. Current evidence supports a model in which each of these pairwise interactions occurs within a large signaling complex.[9]

LRR Domain Models

The crystal structures of the LRRs from the TLR1/TLR2[19] and TLR6/TLR2[20] complexes bound to lipopeptide, the TLR4 dimer bound to myeloid differentiation protein-2 (MD-2) and lipopolysaccharide (LPS),[15] the TLR3 dimer bound to dsDNA,[21] and the TLR5 dimer bound to flagellin[22] have been solved. As a result, it has been possible to predict the structures of the remaining TLRs as well as their ligand binding residues. For example, homology modeling of the TLR9 LRR domain revealed that putative nucleotide binding sites in addition to a number of conserved

BOX 1

COMPUTATIONAL METHODS IN SYSTEMS BIOLOGY

Homology modeling: Known protein structures are used as templates for predicting the structure of a query protein sequence. Such 'template-based' methods are regularly accessed in the Critical Assessment of Techniques for Protein Structure Prediction.[10]

Protein docking: The quaternary structures of protein complexes are predicted from the tertiary structures of the individual component proteins. Challenges include integration of disparate experimental restraints, and predicting conformational changes that occur upon complex formation.[11]

Ordinary differential equations (ODEs): The dynamics of cellular systems are modeled by using biochemical reaction equations such as mass action or Michaelis-Menten kinetics with respect to molecular concentrations. Here, stochasticity inside a cell or heterogeneity of cell population is not considered and systems evolve deterministically.

Stochastic modeling: In a cell, there are several sources of 'noise', which may cause heterogeneity at the population level. Such noise can be modeled by introducing random variables or Monte-Carlo simulation.[12]

Flux balance analysis (FBA): Once stoichiometric coefficients of a biochemical network are known, they impose a constraint on the possible configuration of fluxes at its steady state. FBA determines the optimal fluxes by maximizing a suitably chosen objective function, without requiring knowledge of each kinetic parameter.[13]

Position weight matrix (PWM): PWMs are widely used probabilistic models for sequence motifs in computational biology.[14] In the context of this review, PWMs are used as a model of the DNA-binding preferences of transcription factors, and can be used to predict transcription factor binding sites (TFBSs).

cystine residues that were shown by site-directed mutagenesis to be essential for TLR signaling.[23] Several studies have investigated the ligand binding properties of other TLRs computationally.[24–26] In one such study, homology modeling in combination with generation of LRR/TIR chimeras showed that, like TLR1, TLR10 can bind to TLR2 and has a putative lipopeptide binding site, but that the downstream signaling pathways facilitated by interaction with the TIR domains differ.[24]

TIR Domain Models

A complete structural level understanding of the TIR–TIR interactions that mediate the specific downstream signaling pathways remains elusive, although a number of important advances toward this goal have been made recently. For example, homology modeling indicated that the homodimerization interface of the TLR4 TIR domains is similar to that of TLR10 (Figure 2), which involves pairing of two so-called BB loops, and that this homodimer interface creates a new interface for TIRAP or TRAM (TRIF-related adaptor molecule) binding.[6,7] However, one protein docking study (Box 1) resulted in TIRAP binding to two symmetry-related sites on TLR4,[7] whereas a more recent model supported by the sequence conservation and reporter assays in mammalian cells, places two TIRAP molecules adjacent to each other.[6] The crystal structure of TIRAP has been solved, and is predicted to form a twofold symmetric homodimer.[8] However, two models of TIRAP-MyD88 heterodimerization have been proposed: one in which two TIRAP TIR molecules interact with a single MyD88 TIR domain,[18] and the other in which two MyD88 TIR domains bind to opposite sides of the TIRAP homodimer.[8] The latter model is consistent with the observation that residue D96 in TIRAP and R196 in MyD88 are important for the MyD88-TIRAP interaction.[8] The difficulty in experimentally determining quaternary structures of TIR domain complexes is partially due to their weak binding affinities. This, in turn, means that computational approaches, such as protein docking, in combination with site-directed mutagenesis and protein–protein interaction assays, are expected to play an important role in elucidating the structures of transient signaling complexes.

Death Domain Models

Recently, an X-ray crystallography study revealed the structure of a helical myddosome complex composed of the DDs of MyD88, IRAK-4, and IRAK-2.[27] The myddosome contains 4-6 MyD88 DDs, and 4 DDs each from IRAK-4 and IRAK-2. While it has not yet been determined whether the helical myddosome is present *in vivo*, the authors argue that the 4-6 MyD88 DDs in the myddosome structure suggest a higher-order clustering of TLR dimers, possibly localized on lipid rafts.[9] It is expected that further experiment along with structural modeling will clarify what implications the proposed myddosome complex has for spatial arrangement of upstream TIR and LRR complexes.

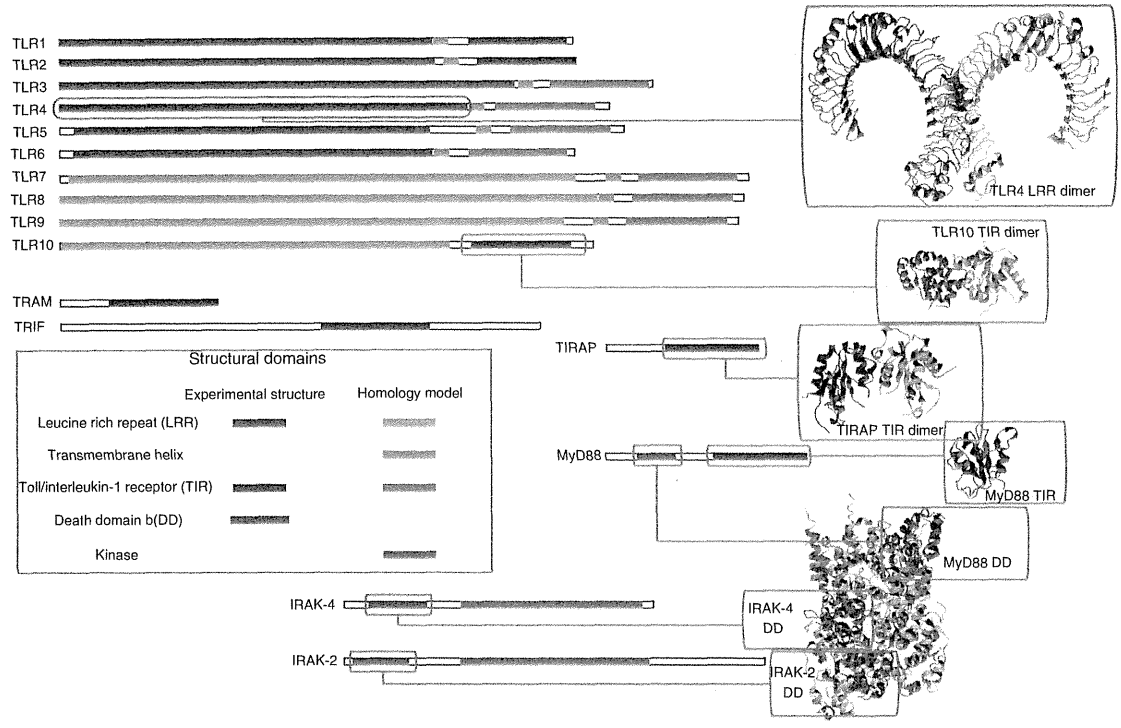

FIGURE 2 | Structural domains of toll-like receptors (TLRs) and their adaptors. The canonical domains of TLRs and their adaptors are shown as 1D bar graphs with the domains drawn to scale. Darker colors indicate experimentally determined structures while lighter colors indicate domains that can be modeled by homology. The cartoon representations of several representative structures are drawn to scale: TLR4 leucine rich repeat (LRR) dimer,[15] TLR10 TIR (interleukin-1) receptordimer,[16] TIRAP TIR dimer,[17] MyD88 TIR,[18] and myddosome complex.[9] In the cartoon representations, dark/light shades are used to distinguish individual chains in dimers.

As the above examples show, structural models provide a framework for understanding the details of macromolecular interactions in terms of their geometry and physical properties. In order to understand the biology of such interactions we need look at larger systems of molecules.

INFERENCE OF TLR SIGNAL TRANSDUCTION NETWORKS

Mathematical Models of Signal Transduction Networks

Mathematical modeling of TLR signal transduction networks allows us to ignore the internal details of each macromolecule in order to focus on their system-level interactions (Figure 3). Early work in this direction focused on integrating data from small-scale experiments. For example, Hoffmann and coworkers[28] constructed a biochemical model of the NF-kB (nuclear factor κ-light-chain-enhancer of activated B cells)/IkB (NF-kB inhibitor) module, which is an important component of the downstream of TLR pathway. Their model is a large set of ordinary differential equations (ODEs, Box 1) based on biochemical parameters derived from cell population averages. They showed that, among three isoforms of IkB (IkBα, IkBβ, and IkBε), IkBα participates in a strong negative feedback loop, which results in oscillatory behavior of NF-kB upon tumor necrosis factor-α (TNFα) stimulation, while the other two isoforms dampen the oscillation. They have also observed similar oscillatory behavior of NF-kB upon LPS stimulation in MyD88 or TRIF deficient mice.[29] In subsequent papers,[30,31] they hypothesized that the temporal patterns of IKK (IkB kinase) activation, which leads to the phosphorylation of IkB and the activation of NF-kB, encode ligand-specific information of upstream signaling. On the basis of this hypothesis, they have modeled the NF-kB activation upon TNFα or LPS stimulation based on experimentally measured IKK activity patterns. These examples illustrate that it is possible to infer the function of molecules through mathematical models, which would be difficult if not impossible experimentally. Details of such models and related works were nicely summarized in Ref 32. It is worth noting, although, that predictions by ODE models in general largely depend on the chosen kinetic

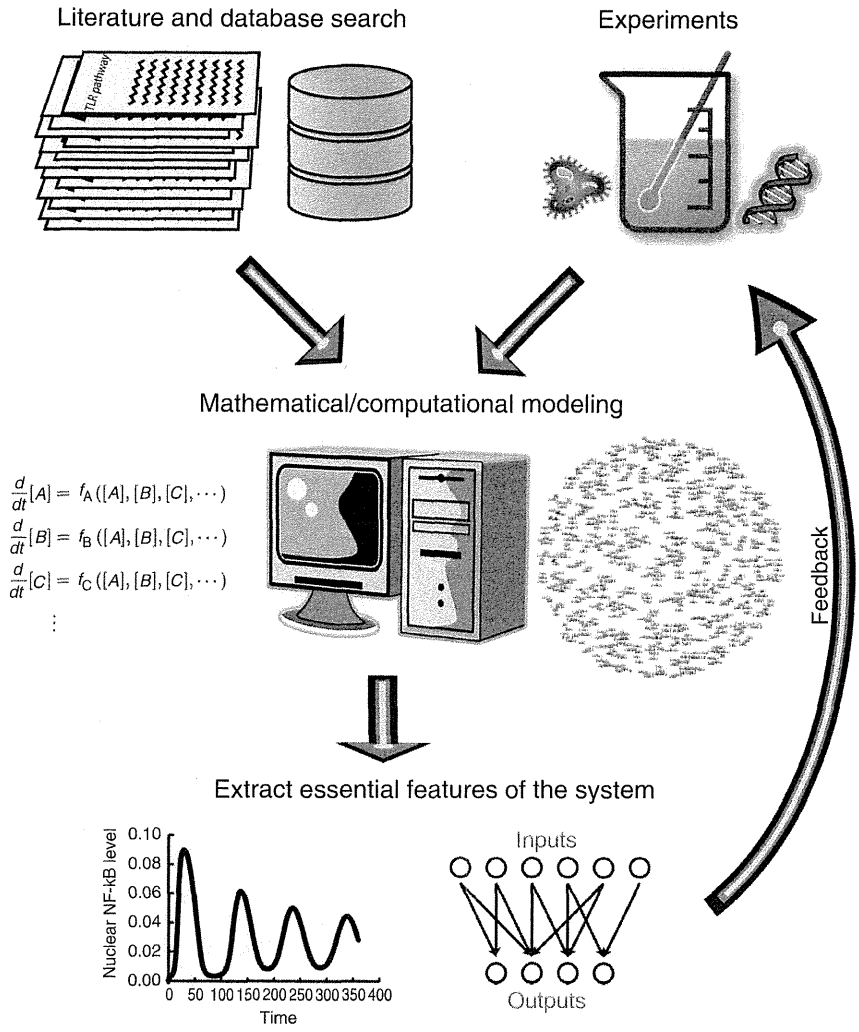

FIGURE 3 | Schematic picture of mathematical modeling approaches to toll-like receptor (TLR) signal transduction networks. In order to construct mathematical models, several kinds of data, such as network topology and biochemical parameters, are required. Those data must be collected or inferred from literature, databases, or experiments. Mathematical models allow us to predict system behavior under different conditions based on assumed rules (or laws). Essential features of the system, such as oscillatory behavior caused by the strong negative feedback loops of IkBa or input–output relationships among TLR receptors and transcriptional output, can be extracted through such models. Predictions can be validated using further experiments, thus enhancing our knowledge of the system.

parameters. In the above models, the authors made great efforts to collect data from the literature as well as through their own experiments. However, it is debatable whether, in the context of ODEs, one can simply integrate data obtained in different cellular contexts or parameters obtained from different models. Nevertheless, even imperfect ODE models provide the basis for further refinement. It is equally important to seek modeling methods that tolerate integration of data and parameters from various contexts, as discussed in Ref 33. Alternatively, approaches that do not require predetermined kinetic parameters can yield important insights, as discussed below.

Another early milestone in systems-level analysis of TLR signaling networks was carried out by Oda and Kitano in 2006.[34] They constructed a comprehensive map of known TLR signaling components based on literature searches. The map revealed a bow-tie structure, where divergent input signals flow into the MyD88 'core' of the network and branch out to multiple components, with much crosstalk with a few collateral pathways. More recently, Li and coworkers[35] analyzed a large-scale TLR signaling pathway using flux balance analysis (FBA, see Box 1), which has origins in the field of metabolic networks. They modified the original Oda-Kitano TLR map to meet FBA

